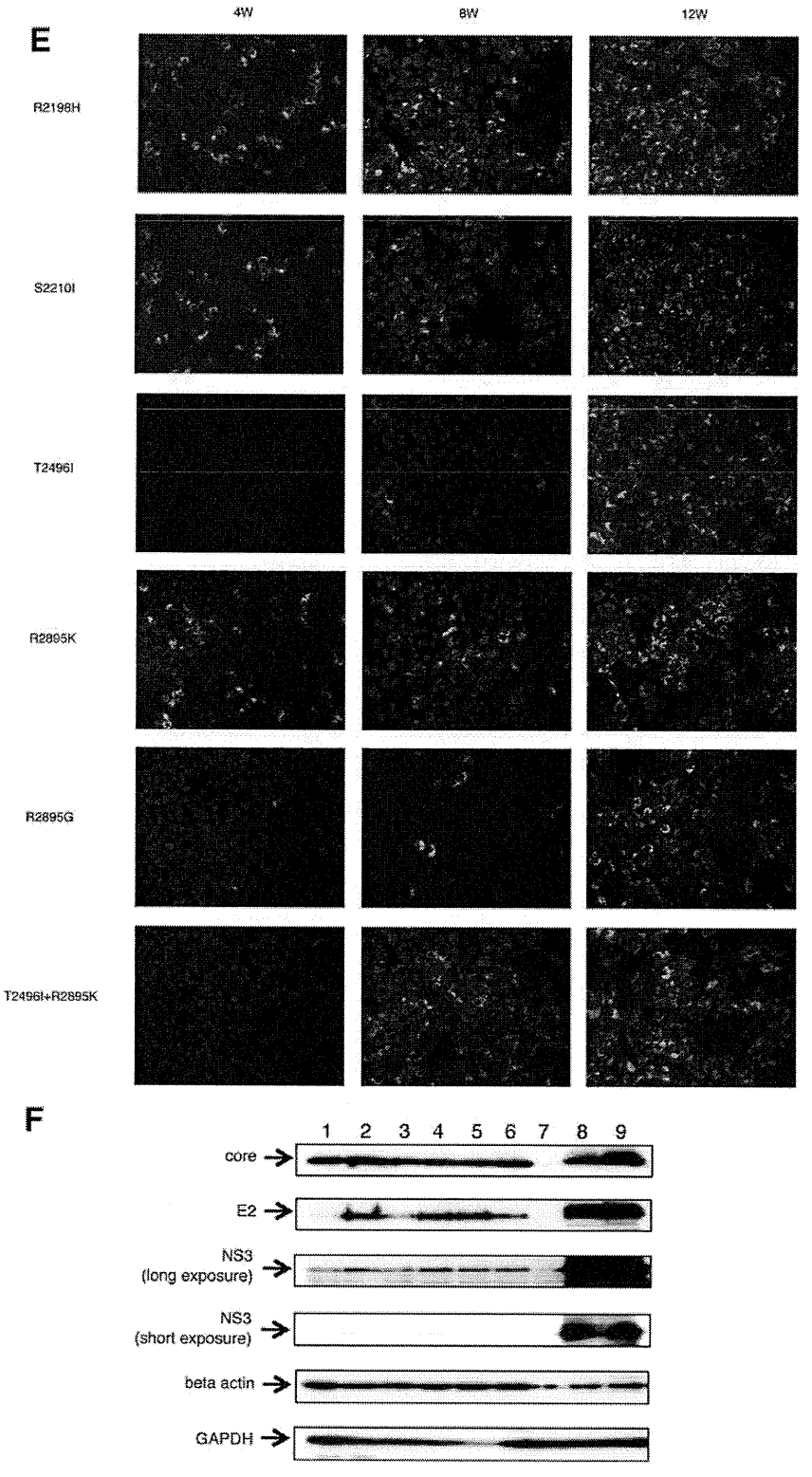

COLOR

Fig. 1. (Continued)

did not secrete any HCV core protein during the observation period. We also determined the HCV RNA levels and infectivity in the culture medium at 4, 8, and 12 weeks after transfection (Fig. 1C,D). The three clones with adaptive mutations (R2198H, R2210I, and R2895K) had higher HCV RNA levels and infectivity than the other clones at 4 weeks after transfection, and their levels increased at 8 and 12 weeks after transfection. The other three clones (T2496I, R2895G, and T2496I + R2896K) had lower levels of HCV RNA and infectivity at 4 weeks after transfection, but from 8 weeks after transfection their levels were similar to the levels of the former three clones. To analyze the mechanism of this discrepancy, we determined the sequences of culture medium of six S310 clones 82 days after transfection (D82) (Table 1). Interestingly, two clones (S2210I and R2895K) that started to secrete infectious virus at earlier timepoints did not have amino acid mutations. R2198H also started to secrete infectious virus at earlier timepoints, although the virus genome had mutations in the E2 and NS3 regions (Table 1). These mutations may be necessary to produce infectious virus in this clone, but we found different mutations in the R2198H virus in an independent repeated experiment (data not shown). The virus genomes of the three other clones (T2496I, R2895G, and T2496I + R2896K) had several mutations in the E2, NS3, NS4B, NS5a, or NS5B regions (Table 1).

T1

Table 1. Sequence Analysis and Neutralization With AP33 Antibody of Culture Medium of 82 Days After Transfection

S310 Clone	Amino Acid Mutations	Regions	AP33 IC_{50} (μg/mL)
R2198H	T416A	E2	0.0514
	H579R	E2	
	A1071V	NS3	
	K1412Q	NS3	
	H1967N	NS4B	
S2210I	ND	-	0.0472
T2496I	T416S	E2	0.0642
	A1071V	NS3	
	D1281N	NS3	
	V1756L	NS4B	
	R2895K	NS5B	
R2895K	ND	-	0.0747
R2895G	I1817V	NS4B	0.0615
	G2895A	NS5B	
	T2999S	NS5B	
T2496I + R2985K	T416N	E2	0.0413
	G2326A	NS5A	
	S2357L	NS5A	
	C2429R	NS5A	

ND, not detected.

To examine whether the replicating virus in the transfected cells could spread to the surrounding cells, the passaged transfected cells were immunostained with anti-core monoclonal antibody (Fig. 1E). We found a greater number of positive cells in three of the clones (R2198H, R2210I, and R2895K), even at 4 weeks after transfection, compared to the others, and the numbers of positive cells increased at 8 and 12 weeks after transfection. On the other hand, the other three clones (T2496I, R2895G, and T2496I + R2896K) began to get more infected at a later timepoint (8 weeks after transfection), and they showed similar numbers of positive cells at 12 weeks after transfection.

Viral protein expression in the S310-transfected cells was detected by western blotting (Fig. 1F). The core protein expression levels were similar in S310 RNA-transfected cells as compared with JFH-1 and J6/JFH1. However, E2 and NS3 protein expression levels were lower than for JFH-1 and J6/JFH1, probably due to the lower affinity of these antibodies to genotype 3a virus. We failed to detect any other NS proteins with the available antibodies. Interestingly, lower E2 protein expression levels were found in lanes 1, 3, and 6 than in the other lanes, although there were no such differences in core protein expression levels. By the sequencing analysis of the virus genome, R2198H, T2496I, and T2496I + R2895K, which had the weaker E2 signals in western blotting, each had a nonsynonymous substitution at amino acid position 416 (R2198H; T to A, T2496I; T to S, T2496I+R2895G; T to N, respectively). This position is located in the epitope of AP33, the anti-E2 antibody. The other three clones (S2210I, R2895K, and R2895G) did not have mutations in the E2 region. Therefore, it appeared that the E2 mutations might disturb antibody binding to E2 protein. To confirm whether neutralization of AP33 was affected by T416 mutations, we determined the 50% inhibitory concentrations (IC_{50}) of AP33 neutralization for each mutant virus clone. However, all clones had similar IC_{50} values (Table 1). Thus, mutations in the anti-E2 antibody epitope region influenced the results of the western blotting assay but not the neutralization assay.

To examine the viral replication and production levels at the late stage of the long-term culture, the HCV core protein levels, RNA levels, and infectivity of the cell culture medium collected 82 days after transfection were determined (Table 2).{TBL2} HCV core protein levels, RNA levels, and infectivity of the six S310 clones were at approximately one-tenth of the levels of the JFH-1 wild-type virus. However, these levels of infectivity (~1,000-6,000 ffu/mL) might be sufficient to maintain secreted S310 virus production

T2

Table 2. Quantification of HCV Core Protein Level, RNA Level, and Infectivity of Culture Medium of 82 Days After Transfection

Mutations	Core (fmol/L)	RNA (copy/ml)	Infectivity (ffu/ml)
R2198H	2,652	1.80E+07	1,000
S2210I	3,334	8.80E+07	4,167
T2496I	3,496	4.33 E+07	2,708
R2895K	4,716	7.83 E+07	6,042
R2895G	1,763	4.11 E+07	417
T2496I+R2895K	2,728	6.26 E+07	1,806
JFH-1	20,932	3.34 E+08	34,722
J6/JFH1	83,388	2.08 E+08	72,917

and replication, since S310 clones could continuously produce the infectious virus in long-term culture (Fig. 1).

Characterization of Cell Culture-Adapted S310 Virus. To characterize the secreted infectious viral particles, we analyzed the culture medium of four S310 clones (R2198H, S2210I, R2895K, and T2496I+ R2895K) by sucrose density gradient centrifugation. HCV particles produced in cell culture with the S310 clones showed major peaks of HCV core protein, RNA, and infectivity at 1.15 mg/mL (Fig. 2). JFH-1 also exhibited similar profiles of HCV core proteins and RNA, but the peak infectivity titers were usually located in a lighter fraction.[18,26] The locations of the peak infectivity titers of S310 clones were different from JFH-1.

S310 viruses (D82), JFH-1 wild-type virus, and J6/JFH1 virus were inoculated into Huh7.5.1 cells at a multiplicity of infection (MOI) of 0.3. To determine whether the cells were successfully infected, we determined and compared the intracellular and extracellular core protein levels of S310 viruses with JFH-1 and J6/JFH1 virus at 24, 48, and 72 hours after infection. Both the intracellular and extracellular core protein levels of all S310 viruses were similar to the levels of JFH-1 wild-type virus, but lower than the levels of J6/JFH1 chimeric virus (Fig. 3A,B). We also evaluated HCV RNA levels and obtained similar results with HCV core protein levels (data not shown). F3

Next, we determined the neutralization of the infection of these viruses by using anti-CD81 antibody (JS81). Anti-CD81 antibody treatment inhibited the infection of Huh7.5.1 cells by ~99% as compared to control IgG (Fig. 3C,D). S310 virus infection was also inhibited by AP33 anti-E2 antibody (Table 1). It is thus suggested that the S310 viruses utilize similar

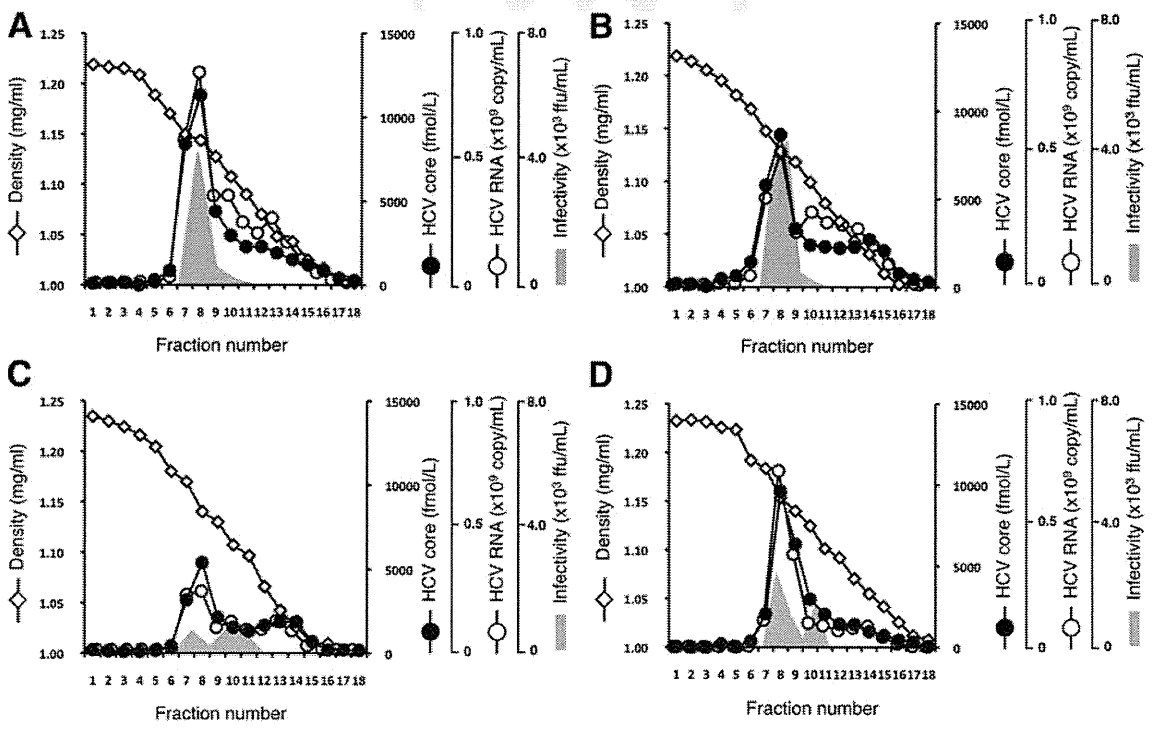

Fig. 2. Sucrose density gradient analysis of the culture medium at 8 weeks after transfection. (A) R2198H, (B) S2210I, (C) R2895K, (D) T2496I+R2895K. Culture medium was overlaid on the stepwise sucrose density gradient (0%, 10%, 20%, 30%, 40%, 50%, and 60% sucrose) and centrifuged for 18 hours at 35,000g at 4°C. A total of 18 fractions were collected from the bottom of the tubes, and density, HCV core protein level, HCV RNA level, and infectivity in each fraction were determined.

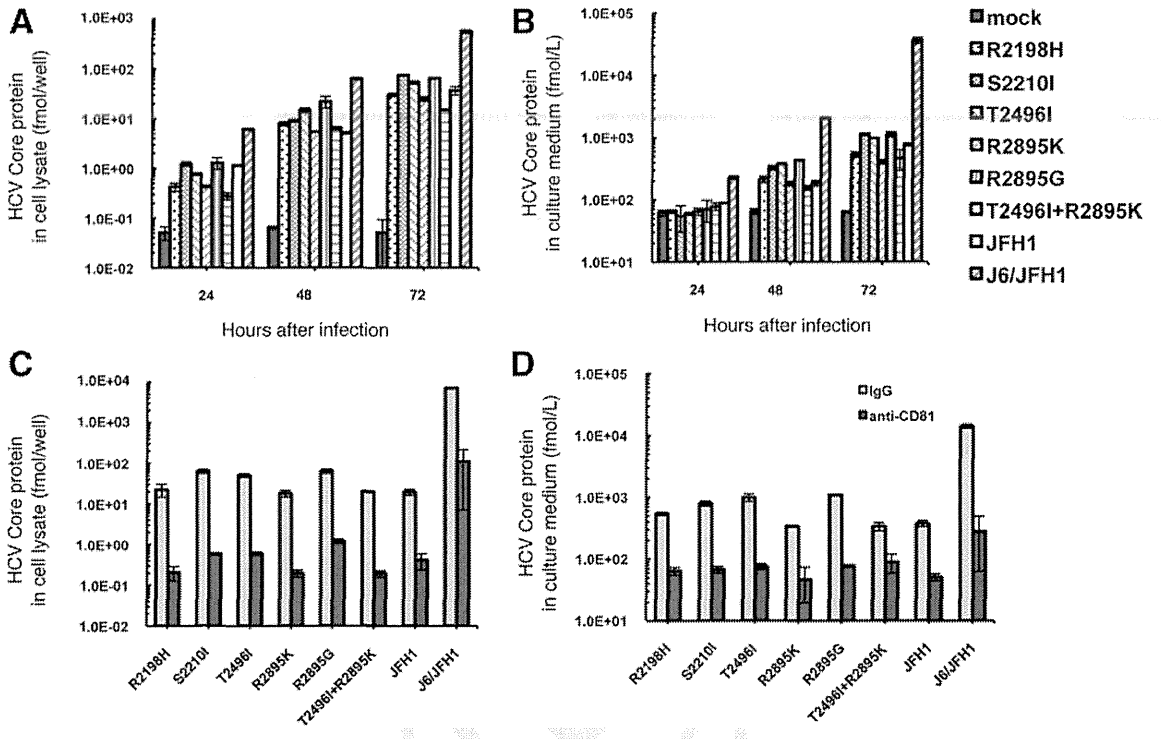

Fig. 3. Comparative analysis with the S310 viruses, JFH-1 and J6/JFH1. (A), (B) Huh7.5.1 cells were infected with the S310 viruses, JFH-1 and J6/JFH1, at an MOI of 0.3. HCV core protein levels in the cell lysate (A) and culture medium (B) were measured at 24, 48, and 72 hours after infection. (C,D) Infection with the adapted S310, JFH-1, and J6/JFH1 virus particles was inhibited by adding anti-CD81 antibody. IgG: normal human immunoglobulin G, anti-CD81: monoclonal anti-CD81 antibody. All assays were performed in triplicate, and data are presented as means ± standard deviation.

infection pathways as JFH-1 and J6/JFH1 chimeric virus, at least with respect to CD81.

To clarify the pathogenesis of genotype 3a infection, cellular sublocalization of HCV core protein and LDs in the S310-infected cells was performed with confocal microscopy. We synthesized RNA of three S310 clones (R2198H, S2210I, and R2895K), S310/JFH1 chimera, and JFH-1 and transfected the synthesized RNA into Huh7.5.1 cells. The cells were passaged every 3-5 days, and passaged cells were seeded onto a slide glass. We used BODIPY, a marker for LDs. S310-derived core proteins showed punctate patterns instead of ring-like patterns and were mainly found in the cytoplasm (Fig. 4A). S310-derived core proteins were not located around the LDs. By contrast, in the JFH-1 virus-infected cells, core proteins colocalized with LDs and exhibited ring-like patterns corresponding to the surfaces of LDs, as previously reported (Fig. 4A).[27] To confirm the intracellular localizations of HCV core protein and LDs, we magnified a partial area of each image and displayed the intensity of both fluorescences (Fig. 4B). We selected the representative region of interest (ROI1) and drew a line in each image. Intensity profiles along the line are shown on the right of the images, and red and green lines indicate the fluorescence intensities of HCV core protein and LDs, respectively. Figure 4B demonstrates that S310-derived core proteins were localized in the cytoplasm and not around the LDs, whereas JFH-1-derived core proteins were colocalized around the surfaces of LDs. These results suggest that the virus particle production pathway may be different between S310 and JFH-1 viruses.

Next, we quantified the lipid content in the infected cells. JFH-1 wild-type virus, S310 viruses (S2210I, T2496I, and R2895K) and S310/JFH1 chimeric virus were inoculated into Huh7.5.1 cell cultures at an MOI of 0.2. Inoculated cells and Huh7.5.1 cells were passaged every 3-5 days. After 11 times of serial passages, core protein, LDs, and nuclei were visualized in the cells. Representative cell images are shown in Fig. 5A. Core proteins (red) were more strongly stained in JFH-1 and S310/JFH1 virus-infected cells than in S310 virus-infected cells, and no core protein staining was observed in Huh7.5.1 cells. The LD staining (green) in the virus-infected cells was higher than in

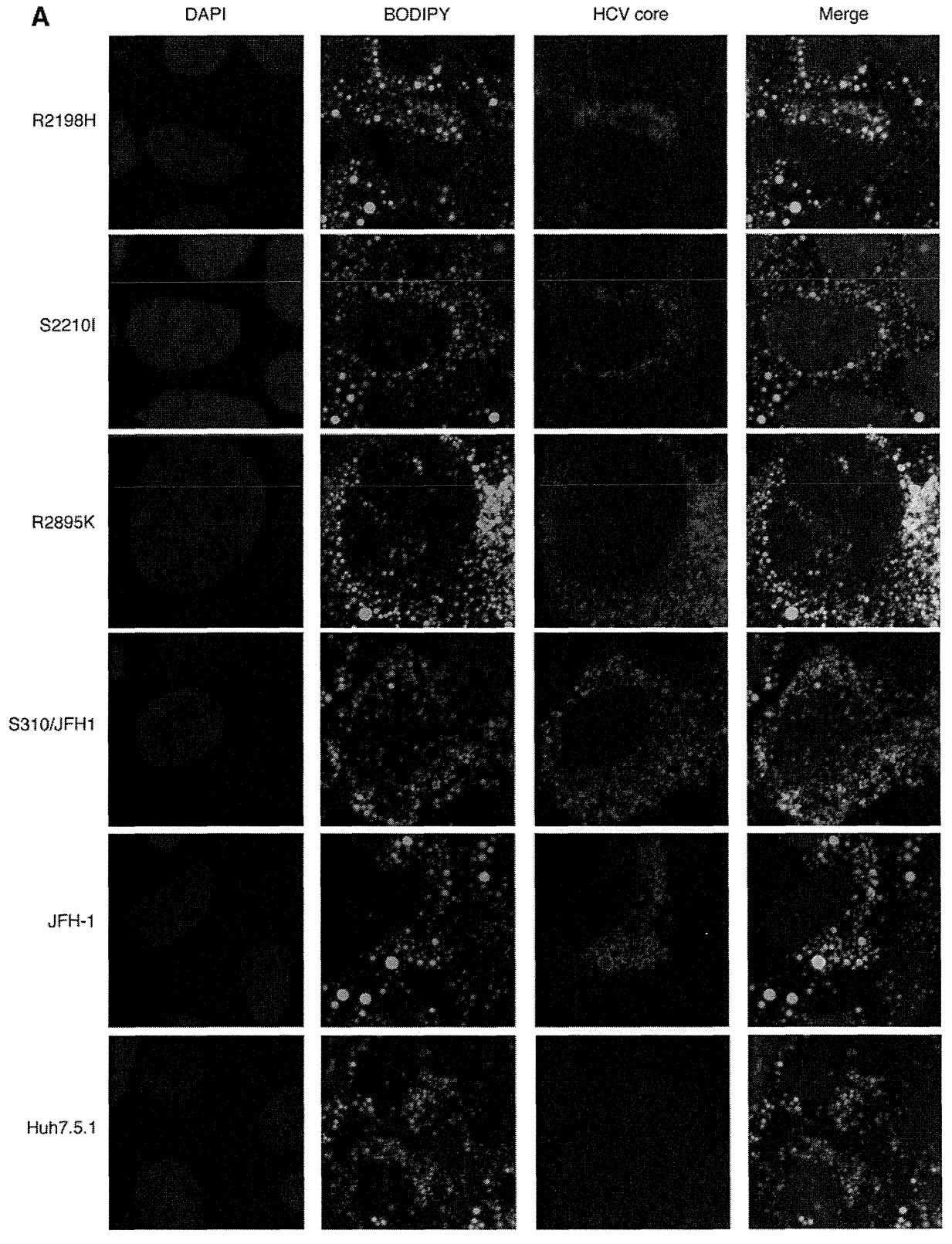

COLOR

Fig. 4. Localization of HCV core proteins and lipid droplets. (A) Huh7.5.1 cells were transfected with the transcribed RNA from each construct. The cells were passaged every 3-5 days, and passaged cells were seeded onto a slide glass. The cells were fixed, probed with the core-specific antibody (red), BODIPY for lipid droplets (green), and DAPI for nucleus staining (blue), and examined by confocal microscopy. Cells at 61 days after transfection are shown. (B) Each merged image was magnified and a line was drawn across the region of interest (ROI1). Intensity profiles along the line are shown on the right of the images. The red line indicates the fluorescence intensity of HCV core protein, and the green line indicates the fluorescence intensity of LDs. The *y*-axis indicates arbitrary units of fluorescence intensity.

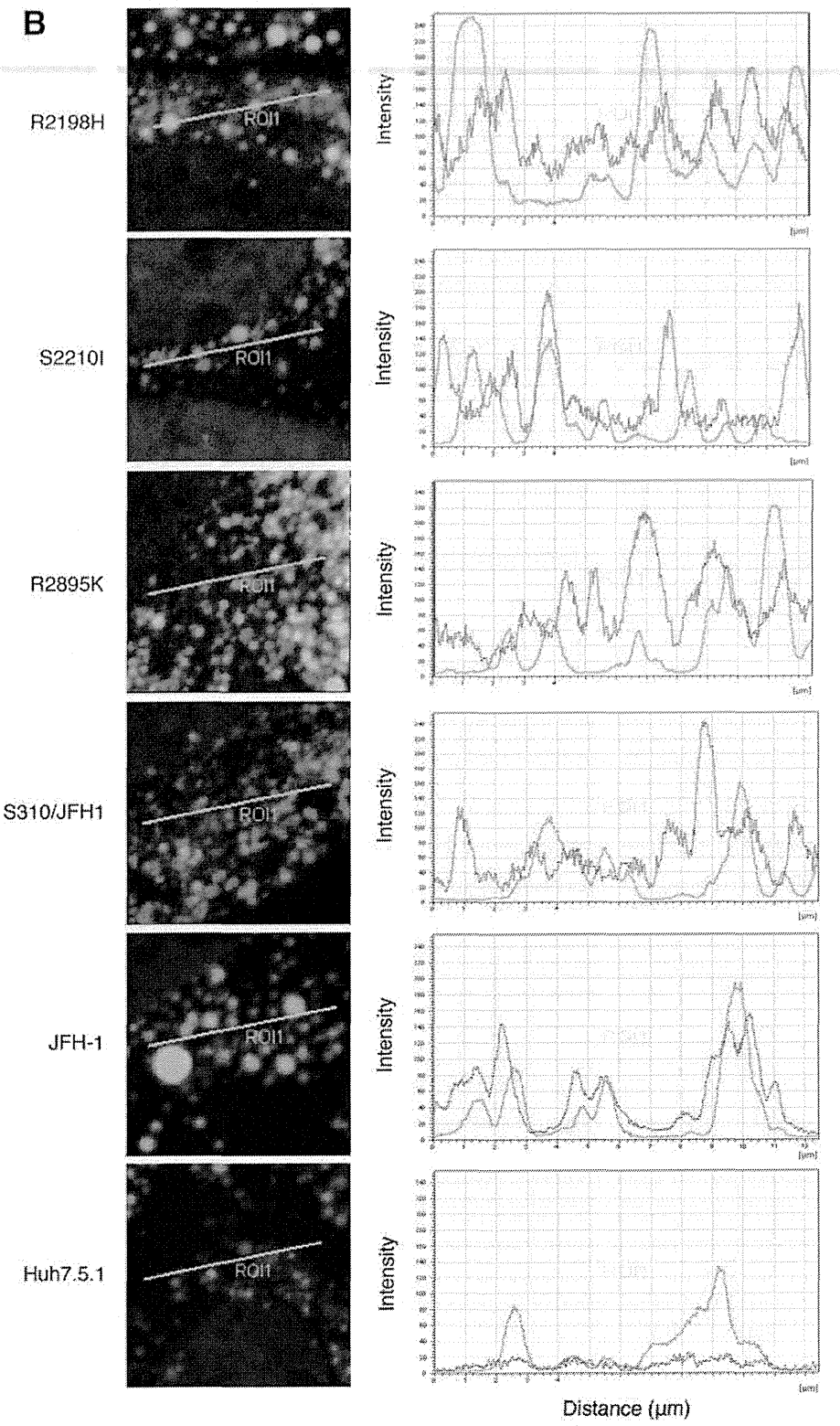

COLOR

Fig. 4. (Continued)

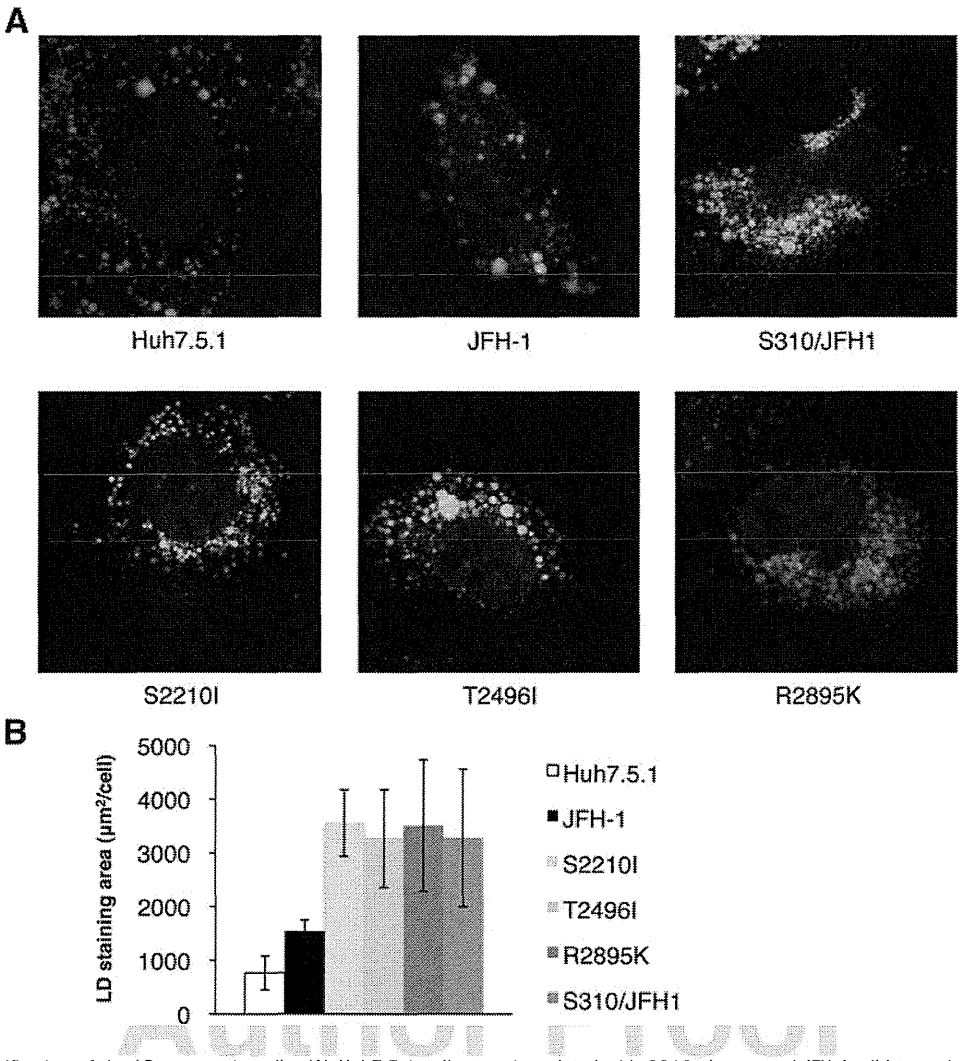

C O L O R

Fig. 5. Quantification of the LD content in cells. (A) Huh7.5.1 cells were inoculated with S310 viruses and JFH-1 wild-type virus at an MOI of 0.2. After 11 serial passages, the cells were analyzed as described in the Fig. 4A legend. (B) The mean values of the LD staining area in 7 cells (from Huh7.5.1 cells and JFH-1 infected cells) or 11 cells (from S310 and S310/JFH1 infected cells) were measured by MetaMorph analysis for each Huh7.5.1 cells and virus-infected cell. The *y*-axis indicates LD staining area. Mean values ± standard deviations are shown.

Huh7.5.1 cells. Furthermore, the LD staining area in the S310 virus (S2210I, T2496I, and R2895K)- and S310/JFH1-infected cells was further greater than in JFH-1-infected cells (Fig. 5A). For the statistical analysis, we selected representative similar sized cells and measured the LD staining area in a single cell by MetaMorph analysis. We analyzed seven cell images each from Huh7.5.1 cells and JFH-1, and 11 cell images each from S310/JFH1 and S310 virus-infected cells. JFH-1 infected cells exhibited significantly higher LD staining levels than Huh7.5.1 cells ($P < 0.0005$). S310 virus and S310/JFH1 chimeric virus-infected cells exhibited significantly much higher LD staining levels than Huh7.5.1 cells ($P < 0.0001$) and than JFH-1 infected cells ($P < 0.005$).

Antiviral Drug Activities Against S310 Viruses. We tested several antiviral drugs against S310 (genotype 3a) and JFH-1 (genotype 2a) infections. In the preliminary experiments, secreted HCV core protein levels were detected in parallel with intracellular HCV RNA levels. We thus used the secreted HCV core protein level as a marker of antiviral activity and determined IC_{50} values against HCV replication (Table 3). Huh7.5.1 cells were inoculated with S310 and JFH-1 viruses at an MOI of 0.2 with or without NS3 protease inhibitor (VX-950), nucleoside polymerase inhibitor (PSI-6130), nonnucleoside polymerase inhibitor (JTK-109), NS5A inhibitor (BMS-790052), CsA, and IFNα. We selected the three S310 viruses (S2210I, T2496I, and R2895K) with NS3, NS5A, or

T3

Table 3. Antiviral Drug Activities Against HCV Infection

	VX-950 (nM)	BMS-790052 (pM)	PSI-6130 (μM)	JTK-109 (μM)	CsA (μM)	IFN-α (IU/mL)
JFH-1	31.2 ± 18.7	20.0 ± 16.8	3.4 ± 1.7	8.7 ± 2.1	0.5 ± 0.2	0.1 ± 0.1
S2210I	9841.0 ± 1026.1	48.1 ± 59.1	1.4 ± 0.1	0.7 ± 0.1**	0.2 ± 0.1	4.2 ± 4.0
T2496I	436.6 ± 81.7*	24.4 ± 23.4	5.6 ± 5.2	2.3 ± 0.6**	0.7 ± 0.6	0.2 ± 0.2
R2895K	436.3 ± 249.8*	10.2 ± 1.7	1.6 ± 0.2	1.4 ± 1.2**	0.9 ± 0.8	4.6 ± 3.7

Assays were performed in triplicate and IC_{50} values are expressed as mean ± standard deviations.
*$P < 0.05$ versus JFH-1.

NS5B adaptive mutations (Table 1). In VX-950 treatment, IC_{50} values for S310 infection seemed to be higher than for JFH-1 infection; however, a statistically significant increase was only observed with T2496I virus infection as compared to JFH-1 virus infection (Table 3). This lack of significance may be due to the large experimental deviation in other S310 virus infections. PSI-6130 inhibited both genotype virus infections at similar levels. However, JTK-109 was significantly more effective against S310 viruses than JFH-1 virus ($P < 0.05$). BMS-790052, CsA, and IFNα inhibited both JFH-1 and S310 viruses at similar levels. There were no differences in antiviral drug efficacies among S310 clones except for VX-950. Adaptive mutations in these three clones may not be important for drug efficacies. Cell viability was determined by the WST-1 assay, and there was no cellular toxicity within the tested dose of the drugs (data not shown).

Discussion

In the present study we established a cell-culture-adapted genotype 3a infectious virus system. In a previous study, adaptive mutations were important for efficient replication of a genotype 3a subgenomic replicon (S310).[9] Therefore, we introduced these mutations into full-length S310 constructs to determine if these constructs can replicate and produce infectious virus particles in cell culture. Full-length S310 wild-type virus did not exhibit increased intracellular and extracellular core levels. However, some of the full-length S310 viruses with adaptive mutations displayed increased intracellular and extracellular core levels in a transient virus production assay (data not shown). To examine whether these clones could continuously produce infectious viral particles, we passaged the S310 RNA-transfected cells repeatedly and monitored the HCV core protein levels in the culture medium for 3 months. As a result, HCV core protein levels of the three clones with adaptive mutations (R2198H, S2210I, and R2895K) increased soon after the transfection and eventually plateaued. From 6 to 8 weeks after transfection, extracellular HCV core protein levels of the other three clones with adaptive mutations (T2496I, R2895G, and T2496I + R2896K) increased rapidly, and their extracellular core protein levels also reached levels similar to the former three clones. All six clones showed sufficient viral RNA replication, virus production, and infectivity for autonomous virus expansion at the end of culture (D82). By sucrose density gradient analysis, we confirmed that S310 clones exhibited similar profiles of HCV core protein and RNA to JFH-1, but the peak infectivity titers were located in the same fraction as HCV core proteins and RNA. The peak infectivity of S310 clones shifted to the heavier fractions as compared to JFH-1. In a previous study, it was also reported that a particular mutant JFH-1 strain exhibited both HCV RNA and infectivity in the same fraction.[28] In that study, a point mutation (G451R) was identified in the viral E2 protein, and the G451R mutation was speculated to increase the density and infectivity of the virus particles.[29] It is thus possible that E2 proteins of S310 clones also alter the density of infectious viral particles. Upon inoculation of secreted S310 viruses into naïve Huh7.5.1 cells, both intracellular and extracellular core protein levels of infected cells were at levels similar to JFH-1 but less than J6/JFH1. In the neutralization experiment, S310 infections of Huh7.5.1 cells were sensitive to anti-CD81 and anti-E2 antibody treatment. Thus, these results suggest that S310 viruses can replicate efficiently and produce infectious virus particles.

Patients with genotype 3a HCV infections tend to develop hepatic steatosis, an intracellular accumulation of lipids and subsequent formation of LDs in the cytoplasm of hepatocytes.[30] S310-infected patient also showed microvesicular and macrovesicular steatosis both before and after liver transplantation. The LD is an organelle used for the storage of neutral lipids. Hepatic steatosis might be involved in inducing lipid synthesis by activation of SREBP-1 and peroxisome proliferator-activated receptor gamma (PPARγ) or by producing reactive oxygen species.[31-33] Inversely, MTP and PPARα might be involved in decreasing lipid secretion and degradation.[34,35]

In previous studies, cells expressing genotype 3a core protein were used to study the genotype 3a HCV core protein association with steatosis.[11-13] HCV genotype 3a core protein up-regulated the activity of fatty acid synthase promoter.[36] Domain 3 of the HCV core protein was sufficient for lipid accumulation, and specific polymorphisms in the HCV core protein of genotype 3a increased the lipid levels, contributing to steatosis in cultured cells.[11] However, the previous systems used only core protein expression, so they lacked the effects of other viral proteins and the entire viral life cycle. Furthermore, HCV core protein sublocalization on the LD surface is important for infectious virus particle formation.[29] We thus analyzed core protein and LD sublocalization by using the genotype 3a infection system. S310-derived core proteins showed punctate signals rather than the ring-like core protein staining pattern usually seen in JFH-1-infected cells (Fig. 4A). We further examined whether S310 infection resulted in the accumulation of LDs in a long-term culture of infected cells. Interestingly, S310 virus-infected cells exhibited greater LD accumulation than Huh7.5.1 cells and JFH-1 virus-infected cells. In addition, LD accumulation in the S310/JFH1 chimeric virus-infected cells was similar to S310 virus-infected cells. S310/JFH1 chimeric virus consists of the S310-derived structural region and the JFH-1-derived nonstructural region. The result thus suggests that the S310-derived structural region is important for LD accumulation in the S310-infected cells. To examine the gene expression levels important for cellular lipid metabolism, we examined MTP, PPARα, and SREBP-1c mRNA expression by real-time PCR. However, no differences in mRNA expression levels were found in between Huh7.5.1 cells and the infected cells (data not shown). Further detailed analysis will be necessary to clarify the mechanisms for LD accumulation in S310 virus-infected cells.

To provide new therapeutic approaches for genotype 3a HCV infections, we examined the antiviral drug activity against S310-infected cells. In VX-950 treatment, IC_{50} values for S310 infection seemed to be higher than for JFH-1 infection; however, VX-950 was only statistically less effective for T2496I infection as compared to JFH-1 infection. In our previous study, another NS3 protease inhibitor, BILN-2061, was also less effective for the S310 subgenomic replicon as compared to the JFH-1 and Con1 replicons. JTK-109, a nonnucleoside polymerase inhibitor, was more effective for S310 than JFH-1. Other inhibitors, including NS5A inhibitor, nucleoside NS5B inhibitor, IFNα, and CsA, inhibited both viruses at similar levels. Thus, this novel genotype 3a cell culture system can be used to assay possible antiviral compounds.

In conclusion, we established an HCV genotype 3a cell culture system. The patients infected with genotype 3a HCV appear to have different clinical characteristics than patients infected with other genotypes. This genotype 3a infectious cell culture system will be useful for studying the molecular mechanism of HCV viral life cycles and pathogenesis as well as for developing specific antiviral drugs for genotype 3a infections.

Acknowledgment: Huh7.5.1 cells were kindly provided by Dr. Francis V. Chisari. The J6CF plasmid was a kind gift from Dr. Jens Bukh. AP33 antibody was generously provided by Genentech. JTK-109 and PSI-6130 were generous gifts from Japan Tobacco, Inc., and Pharmasset, Inc., respectively.

References

1. Feld JJ, Liang TJ. Hepatitis C — identifying patients with progressive liver injury. HEPATOLOGY 2006;43:S194-206.
2. Smith DB, Bukh J, Kuiken C, Muerhoff AS, Rice CM, Stapleton JT, et al. Expanded classification of hepatitis C Virus into 7 genotypes and 67 subtypes: updated criteria and assignment web resource. HEPATOLOGY 2014;59:318-327.
3. Butt S, Idrees M, Akbar H, ur Rehman I, Awan Z, Afzal S, et al. The changing epidemiology pattern and frequency distribution of hepatitis C virus in Pakistan. Infect Genet Evol 2010;10:595-600.
4. Rehman IU, Idrees M, Ali M, Ali L, Butt S, Hussain A, et al. Hepatitis C virus genotype 3a with phylogenetically distinct origin is circulating in Pakistan. Genet Vaccines Ther 2011;9:2.
5. Hui JM, Kench J, Farrell GC, Lin R, Samarasinghe D, Liddle C, et al. Genotype-specific mechanisms for hepatic steatosis in chronic hepatitis C infection. J Gastroenterol Hepatol 2002;17:873-881.
6. Rubbia-Brandt L, Quadri R, Abid K, Giostra E, Male PJ, Mentha G, et al. Hepatocyte steatosis is a cytopathic effect of hepatitis C virus genotype 3. J Hepatol 2000;33:106-115.
7. Kumar D, Farrell GC, Fung C, George J. Hepatitis C virus genotype 3 is cytopathic to hepatocytes: reversal of hepatic steatosis after sustained therapeutic response. HEPATOLOGY 2002;36:1266-1272.
8. Gottwein JM, Scheel TK, Jensen TB, Ghanem L, Bukh J. Differential efficacy of protease inhibitors against HCV genotypes 2a, 3a, 5a, and 6a NS3/4A protease recombinant viruses. Gastroenterology 2011;141:1067-1079.
9. Saeed M, Gondeau C, Hmwe S, Yokokawa H, Date T, Suzuki T, et al. Replication of hepatitis C virus genotype 3a in cultured cells. Gastroenterology 2013;144:56-58 e57.
10. Saeed M, Scheel TK, Gottwein JM, Marukian S, Dustin LB, Bukh J, et al. Efficient replication of genotype 3a and 4a hepatitis C virus replicons in human hepatoma cells. Antimicrob Agents Chemother 2012;56:5365-5373.
11. Jhaveri R, McHutchison J, Patel K, Qiang G, Diehl AM. Specific polymorphisms in hepatitis C virus genotype 3 core protein associated with intracellular lipid accumulation. J Infect Dis 2008;197:283-291.
12. Jhaveri R, Qiang G, Diehl AM. Domain 3 of hepatitis C virus core protein is sufficient for intracellular lipid accumulation. J Infect Dis 2009;200:1781-1788.
13. Qiang G, Jhaveri R. Lipid droplet binding of hepatitis C virus core protein genotype 3. ISRN Gastroenterol 2012;2012:176728.
14. Lindenbach BD, Evans MJ, Syder AJ, Wolk B, Tellinghuisen TL, Liu CC, et al. Complete replication of hepatitis C virus in cell culture. Science 2005;309:623-626.

15. Pietschmann T, Kaul A, Koutsoudakis G, Shavinskaya A, Kallis S, Steinmann E, et al. Construction and characterization of infectious intragenotypic and intergenotypic hepatitis C virus chimeras. Proc Natl Acad Sci U S A 2006;103:7408-7413.
16. Kato T, Date T, Murayama A, Morikawa K, Akazawa D, Wakita T. Cell culture and infection system for hepatitis C virus. Nat Protoc 2006;1:2334-2339.
17. Wakita T. Isolation of JFH-1 strain and development of an HCV infection system. Methods Mol Biol 2009;510:305-327.
18. Wakita T, Pietschmann T, Kato T, Date T, Miyamoto M, Zhao Z, et al. Production of infectious hepatitis C virus in tissue culture from a cloned viral genome. Nat Med 2005;11:791-796.
19. Saeed M, Suzuki R, Kondo M, Aizaki H, Kato T, Mizuochi T, et al. Evaluation of hepatitis C virus core antigen assays in detecting recombinant viral antigens of various genotypes. J Clin Microbiol 2009;47:4141-4143.
20. Takeuchi T, Katsume A, Tanaka T, Abe A, Inoue K, Tsukiyama-Kohara K, et al. Real-time detection system for quantification of hepatitis C virus genome. Gastroenterology 1999;116:636-642.
21. Date T, Miyamoto M, Kato T, Morikawa K, Murayama A, Akazawa D, et al. An infectious and selectable full-length replicon system with hepatitis C virus JFH-1 strain. Hepatol Res 2007;37:433-443.
22. Kato T, Date T, Miyamoto M, Furusaka A, Tokushige K, Mizokami M, et al. Efficient replication of the genotype 2a hepatitis C virus subgenomic replicon. Gastroenterology 2003;125:1808-1817.
23. Date T, Kato T, Kato J, Takahashi H, Morikawa K, Akazawa D, et al. Novel cell culture-adapted genotype 2a hepatitis C virus infectious clone. J Virol 2012;86:10805-10820.
24. Zhong J, Gastaminza P, Cheng G, Kapadia S, Kato T, Burton DR, et al. Robust hepatitis C virus infection in vitro. Proc Natl Acad Sci U S A 2005;102:9294-9299.
25. Olmstead AD, Knecht W, Lazarov I, Dixit SB, Jean F. Human subtilase SKI-1/S1P is a master regulator of the HCV Lifecycle and a potential host cell target for developing indirect-acting antiviral agents. PLoS Pathog 2012;8:e1002468.
26. Kato T, Matsumura T, Heller T, Saito S, Sapp RK, Murthy K, et al. Production of infectious hepatitis C virus of various genotypes in cell cultures. J Virol 2007;81:4405-4411.
27. Miyanari Y, Atsuzawa K, Usuda N, Watashi K, Hishiki T, Zayas M, et al. The lipid droplet is an important organelle for hepatitis C virus production. Nat Cell Biol 2007;9:1089-1097.
28. Gastaminza P, Dryden KA, Boyd B, Wood MR, Law M, Yeager M, et al. Ultrastructural and biophysical characterization of hepatitis C virus particles produced in cell culture. J Virol 2010;84:10999-11009.
29. Zhong J, Gastaminza P, Chung J, Stamataki Z, Isogawa M, Cheng G, et al. Persistent hepatitis C virus infection in vitro: coevolution of virus and host. J Virol 2006;80:11082-11093.
30. Anderson N, Borlak J. Molecular mechanisms and therapeutic targets in steatosis and steatohepatitis. Pharmacol Rev 2008;60:311-357.
31. Gavrilova O, Haluzik M, Matsusue K, Cutson JJ, Johnson L, Dietz KR, et al. Liver peroxisome proliferator-activated receptor gamma contributes to hepatic steatosis, triglyceride clearance, and regulation of body fat mass. J Biol Chem 2003;278:34268-34276.
32. Videla LA, Rodrigo R, Orellana M, Fernandez V, Tapia G, Quinones L, et al. Oxidative stress-related parameters in the liver of non-alcoholic fatty liver disease patients. Clin Sci (Lond) 2004;106:261-268.
33. Ma S, Yang D, Li D, Tan Y, Tang B, Yang Y. Inhibition of uncoupling protein 2 with genipin exacerbates palmitate-induced hepatic steatosis. Lipids Health Dis 2012;11:154.
34. Perlemuter G, Sabile A, Letteron P, Vona G, Topilco A, Chretien Y, et al. Hepatitis C virus core protein inhibits microsomal triglyceride transfer protein activity and very low density lipoprotein secretion: a model of viral-related steatosis. FASEB J 2002;16:185-194.
35. Mirandola S, Realdon S, Iqbal J, Gerotto M, Dal Pero F, Bortoletto G, et al. Liver microsomal triglyceride transfer protein is involved in hepatitis C liver steatosis. Gastroenterology 2006;130:1661-1669.
36. Jackel-Cram C, Babiuk LA, Liu Q. Up-regulation of fatty acid synthase promoter by hepatitis C virus core protein: genotype-3a core has a stronger effect than genotype-1b core. J Hepatol 2007;46:999-1008.

Supporting Information

Additional Supporting Information may be found in the online version of this article at the publisher's website.

PLOS ONE

Involvement of MAP3K8 and miR-17-5p in Poor Virologic Response to Interferon-Based Combination Therapy for Chronic Hepatitis C

Akihito Tsubota[1,2]*, Kaoru Mogushi[3], Hideki Aizaki[4], Ken Miyaguchi[3], Keisuke Nagatsuma[1,2], Hiroshi Matsudaira[1,2], Tatsuya Kushida[5], Tomomi Furihata[6], Hiroshi Tanaka[3], Tomokazu Matsuura[7]

1 Institute of Clinical Medicine and Research (ICMR), Jikei University School of Medicine, Kashiwa, Chiba, Japan, **2** Division of Gastroenterology and Hepatology, Kashiwa Hospital, The Jikei University School of Medicine, Kashiwa, Chiba, Japan, **3** Department of Bioinformatics, Medical Research Institute, Tokyo Medical and Dental University, Bunkyo-ku, Tokyo, Japan, **4** Department of Virology II, National Institute of Infectious Diseases, Shinjuku-ku, Tokyo, Japan, **5** National Bioscience Database Center, Japan Science and Technology Agency, Chiyoda-ku, Tokyo, Japan, **6** Laboratory of Pharmacology and Toxicology, Graduate School of Pharmaceutical Science, Chiba University, Chiba, Japan, **7** Department of Laboratory Medicine, Jikei University School of Medicine, Minato-ku, Tokyo, Japan

Abstract

Despite advances in chronic hepatitis C treatment, a proportion of patients respond poorly to treatment. This study aimed to explore hepatic mRNA and microRNA signatures involved in hepatitis C treatment resistance. Global hepatic mRNA and microRNA expression profiles were compared using microarray data between treatment responses. Quantitative real-time polymerase chain reaction validated the gene signatures from 130 patients who were infected with hepatitis C virus genotype 1b and treated with pegylated interferon-alpha and ribavirin combination therapy. The correlation between mRNA and microRNA was evaluated using *in silico* analysis and *in vitro* siRNA and microRNA inhibition/overexpression experiments. Multivariate regression analysis identified that the independent variables IL28B SNP rs8099917, hsa-miR-122-5p, hsa-miR-17-5p, and MAP3K8 were significantly associated with a poor virologic response. MAP3K8 and miR-17-5p expression were inversely correlated with treatment response. Furthermore, miR-17-5p repressed HCV production by targeting MAP3K8. Collectively, the data suggest that several molecules and the inverse correlation between mRNA and microRNA contributed to a host genetic refractory hepatitis C treatment response.

Citation: Tsubota A, Mogushi K, Aizaki H, Miyaguchi K, Nagatsuma K, et al. (2014) Involvement of MAP3K8 and miR-17-5p in Poor Virologic Response to Interferon-Based Combination Therapy for Chronic Hepatitis C. PLoS ONE 9(5): e97078. doi:10.1371/journal.pone.0097078

Editor: Wenyu Lin, Harvard Medical School, United States of America

Received December 6, 2013; **Accepted** April 14, 2014; **Published** May 12, 2014

Funding: This work was supported in part by Grants-in-Aid from the Ministry of Health, Labour and Welfare (Japan), the Ministry of Education, Culture, Sports, Science and Technology (Japan), and Clinical Research Funds from ICMR, the Jikei University School of Medicine. The funders had no role in study design, data collection and analysis, decision to publish, or preparation of the manuscript.

Competing Interests: The authors have declared that no competing interests exist.

* E-mail: atsubo@jikei.ac.jp

Introduction

Chronic hepatitis C (CH-C) caused by hepatitis C virus (HCV) infection is a major chronic liver disease worldwide, and it often develops into cirrhosis and hepatocellular carcinoma. Pegylated interferon alpha (peg-IFNα) and ribavirin (RBV) combination therapy is widely used to treat CH-C [1]. However, treatment fails in approximately 50% patients with HCV genotype 1. Of note, approximately 20–30% patients show null or partial response to the treatment. The introduction of nonstructural 3/4A protease inhibitors has improved the outcome for genotype 1 CH-C patients [1]. However, new antiviral agents increase the frequency and severity of adverse effects, are costly, have complex treatment regimens, and often result in viral resistance. Importantly, the outcomes of triple combination therapy are extremely poor in patients who showed null and partial response to previous peg-IFNα/RBV, compared to treatment-naïve patients and relapsers [1–3]. Furthermore, over 50% of null and partial responders, among all patients with a similar virologic response or viral kinetics, relapse after treatment cessation [2,3]. Collectively, these studies suggest a role of host genetics in treatment resistance.

Microarray applications in clinical medicine identified that numerous mRNAs and microRNAs (miRNAs) regulate complex processes involved in disease development. For example, hepatic mRNA expression of IFN-stimulated genes (ISGs, such as ISG15, OAS, IFI, IP10, and viperin) and IFN-related pathway genes (MX and USP18) correlate with responses to peg-IFNα/RBV combination therapy for CH-C [4–7]. However, few studies have examined global miRNAs alone [8]. Furthermore, mRNA and miRNA gene signatures and their interactions in treatment response have not been reported. miRNAs are evolutionarily conserved, small non-coding RNAs [9,10]. A single miRNA can regulate the expression of multiple target mRNAs and their encoded proteins by imperfect base pairing and subsequent mRNA cleavage/translational repression. Conversely, the expression of a single mRNA is often regulated by several miRNAs. As regulators of promotion or suppression of gene expression, miRNAs are involved in diverse biological and physiological processes, including cell cycle, proliferation, differentiation, and apoptosis. In addition to targeting endogenous mRNAs, miRNAs regulate the life cycle of viruses such as the Epstein-Barr virus,

HCV, and other oncogenic viruses by interacting with viral transcripts [11,12].

We investigated the differential expression profiles of mRNAs and miRNAs isolated from the liver tissues of untreated patients with HCV genotype 1b using microarray analysis. Expression profiles and their interactions were analyzed to identify the molecular signatures associated with treatment resistance.

Materials and Methods

Patient population, treatment, and liver tissue samples

During 2010 and 2011, 130 patients infected with HCV genotype 1b were treated weekly with 1.5 μg/kg of peg-IFNα-2b (MSD, Tokyo) and daily with 600–1000 mg RBV (MSD) [2,3] for 48 weeks at Jikei University Kashiwa-affiliated hospitals. Patients with undetectable serum HCV RNA at week 12 or later were recommended to extend the treatment to 72 weeks. All study participants provided informed written consent and materials for genetic testing and met the following criteria: (1) CH-C diagnosis confirmed by laboratory tests, virology, and histology; (2) genotype 1b confirmed by polymerase chain reaction (PCR)-based method; (3) absence of malignancy, liver failure, or other form of chronic liver disease; and (4) no concurrent treatment with any other antiviral or immunomodulatory agent. Liver specimens were obtained percutaneously before treatment, formalin-fixed, and paraffin-embedded for histological assessment [13]. A tissue section was stored in RNA*later* solution (Life Technologies, Carlsbad, CA). Total RNA containing mRNA and miRNA was isolated using the mirVana miRNA isolation kit (Life Technologies).

Sustained virological response (SVR) was defined as an undetectable serum HCV RNA level at 24 weeks after treatment completion. A null response was defined as a viral decline of $< 2\ \log_{10}$ IU/mL from baseline at treatment week 12 and detectable HCV RNA during treatment. A partial response was defined as a viral decline of $>2\ \log_{10}$ IU/mL from baseline at week 12, with no achievement of an undetectable HCV RNA level. Relapse was defined as an undetectable serum HCV RNA level at the end of treatment and viremia reappearance on follow-up examination [1]. Viral loads and the presence or absence of serum HCV RNA were evaluated using a qualitative PCR assay (Amplicor HCV version 2.0; Roche Diagnostics, Tokyo).

This study conformed to the provisions of the Declaration of Helsinki and Good Clinical Practice guidelines and was approved by the Jikei University Ethics Committee for Human Genome/Gene Analysis Research (No.21-093_5671).

mRNA microarray

Global mRNA expression analysis was performed using total RNA isolated from each sample [sustained virological responders (SVRs), $n=5$; relapsers, $n=3$; null responders, $n=4$] and the GeneChip Human Genome U133 Plus 2.0 Array (Affymetrix, Santa Clara, CA). Datasets were normalized by the robust multi-array analysis, using R 2.12.1 statistical software and the BioConductor package.

miRNA microarray

Global miRNA expression analysis was performed using total RNA isolated from the same samples used for mRNA expression analysis and the miRCURY LNA microRNA Array series (Exiqon, Vedbaek, Denmark). Total RNA was labeled with Hy3 and hybridized to slides that contained capture probes targeting all human miRNAs registered in the miRBASE 14.0. miRNA microarray datasets were normalized by quantile normalization using R statistical software.

Differential gene expression according to treatment response

The limma package from BioConductor software (under R statistical software) was used to calculate moderated t-statistics (based on the empirical Bayes approach) to identify mRNA or miRNA differentially expressed between the SVR/relapser group and null/partial responder group. Because of multiple hypothesis testing, p values were adjusted by the Benjamini-Hochberg false discovery rate (FDR) method.

Hierarchical cluster analysis

Up- and down-regulated probe sets were analyzed by hierarchical clustering using R statistical software. Pearson's correlation coefficients were used to calculate a matrix similarity score among the probe sets. The complete linkage method was used for agglomeration. Heat maps were generated from significant differentially expressed probe sets.

Quantitative real-time PCR for mRNA

To validate microarray results and to confirm the observed differences in the mRNA expression levels in a quantitative manner, each sample was subjected to reverse transcription (RT)-PCR and quantitative real-time RT-PCR (qPCR) in triplicate. After cDNA synthesis, target genes were amplified in PCR mixtures that contained TaqMan Universal PCR Master Mix (Life Technologies) and TaqMan probes designed with the Universal Probe Library Assay Design Center (http://www.roche-applied-science.com/sis/rtpcr/upl/adc.jsp). Target gene expression levels in each sample were normalized to the expression of the housekeeping gene of 18S rRNA and the corresponding gene of one null responder.

Quantitative real-time PCR for miRNA

cDNA was synthesized from aliquots of the isolated total RNA using the TaqMan MicroRNA Reverse Transcription kit (Life Technologies) including RT primers designed with miRNA-specific stem-loop structures according to manufacturer's protocol. miRNA expression levels were quantified with the TaqMan MicroRNA assay (Life Technologies) in triplicate. Target gene expression levels were normalized in each sample to the expression of the endogenous gene RNU48 and the corresponding gene of one null responder.

miRNA target prediction

Up- and down-regulated miRNAs with a fold change of >1.2 and $p<0.005$ (FDR<0.15) between two groups (SVRs/relapsers *vs* null responders) in the microarray analysis were subjected to the *in silico* prediction of mRNA targets for miRNA using MicroCosm Targets, miRanda, PicTar, PITA, and TargetScan algorithms. Predicted mRNA targets were analyzed further if they met the following criteria: (1) fold change of >1.5 and $p<0.003$ (FDR$<$ 0.35) in mRNA microarray results; (2) inverse correlation (negative correlation coefficient) between miRNA and mRNA in mRNA and miRNA microarray results; and (3) qPCR-validated microarray results. Kyoto Encyclopedia of Genes and Genomes (KEGG) Pathways, Agilent Literature Search 3.0.3 beta, and Cytoscape 3.0.2 were used to identify the significance of candidates in gene regulatory networks.

Cell culture

The human hepatoma cell line Huh7.5.1 (a gift from Professor Francis Chisari, Scripps Research Institute, La Jolla, CA) was maintained in Dulbecco's modified Eagle's medium containing 10% fetal bovine serum [14]. Cell culture-produced HCV (HCVcc) were harvested from JFH1-transfected Huh7.5.1 as previously described [15].

Plasmids and siRNAs

The siRNAs targeting MAP3K8 were siRNA1, 5′-uucgucuuuauaucuugugtt-3′; siRNA2, 5′-uguugcuagguuuaauauctt-3′; siRNA3, 5′-aucuugugccaaguauacctt-3′; and scrambled negative control siRNA to siRNA1 (Sigma-Aldrich, St. Louis, MO). The expression and inhibitor plasmids of hsa-miR-17-5p and control plasmids were purchased from GeneCopoeia (Rockville, MD).

HCV core antigen measurements and cell viability

The HCV core antigen concentrations in filtered culture medium and cell lysates of infected cells were measured with the Lumipulse Ortho HCV antigen kit (Ortho Clinical Diagnostics, Tokyo). Cell viability was analyzed using the CellTiter-Glo Luminescent Cell Viability Assay (Promega, Madison, WI).

Transfection

Cells were seeded into a 24-well plate and transfected with siRNAs and plasmids using Lipofectamine RNAiMAX (Invitrogen, San Diego, CA) and TransIT-LT1 (Mirus, Madison, WI), respectively.

Luciferase reporter assay

The MAP3K8 3′UTR segment containing the putative miR-17-5p target sites was subcloned into the pGL3 reporter plasmid (Promega). A mutant construct was also generated by PCR-based mutagenesis using mutagenic primers. The luciferase reporter and hsa-miR-17-5p expressing or mock plasmids were co-transfected with the *Renilla* luciferase transfection control plasmid. Luciferase reporter activity was measured 48 hours after transfection with the Dual-Luciferase Reporter Assay System (Promega).

Western blot

Liver samples were sonicated in lysis buffer. Lysate aliquots were separated by SDS-polyacrylamide gel electrophoresis and transferred onto a nitrocellulose membrane. Membranes were incubated with primary antibodies against MAP3K8 (ab70853, Abcam, San Diego, CA) and β-actin (EP1123Y, Abcam). Membranes were incubated with horseradish peroxidase-conjugated secondary antibodies. Immunoreactivity was detected with reagents (GE Healthcare Life Sciences, Piscataway, NJ). Images were scanned and band intensities quantified with Image J.

IL28B and ITPA single nucleotide polymorphism (SNP) genotyping

Genomic DNA was extracted from whole blood using the MagNA Pure LC and the DNA Isolation Kit (Roche Diagnostics). The IL28B rs8099917 and rs12979860 [16,17] and ITPA exon 2 rs1127354 [18] genetic polymorphisms were genotyped by real-time detection PCR with the TaqMan SNP Genotyping Assays.

Statistical analysis for factors associated with null/partial response

The chi-square, Fisher's exact, Student's *t*, and the Mann–Whitney two-tailed tests were used to compare frequencies in categorical data or differences in continuous data between two groups. Significant independent factors associated with null/partial responses were identify with multiple logistic regression analysis using the SPSS statistical package for Windows, version 17.0 (IBM SPSS, Chicago, IL). A p value of <0.05 was considered statistically significant.

Results

Patient profiles and treatment response

Among the 130 patients, 62 (48%) achieved SVR, 36 (28%) relapsed, and six (5%) and 26 (20%) showed partial and null response, respectively. Patients were divided into an SVR/relapser group and a null/partial responder group. Table S1 compares the baseline characteristics of the two groups. Patients with elevated serum gamma glutamyl transpeptidase and decreased albumin concentrations were more likely to experience a null/partial response. The IL28B rs8099917 TG and rs12979860 CT variants were more likely to be null/partial responders compared with TT and CC genotypes, respectively.

mRNAs associated with treatment response

mRNA microarray data were deposited into the NCBI Gene Expression Omnibus (GEO) (http://www.ncbi.nlm.nih.gov/geo/), accession number GSE42697. The cut-off criteria for fold change >1.5 and $p<0.003$ identified 39 up-regulated and 17 down-regulated annotated probe sets in null responders (Data S1). The up-regulated genes were associated with transcription, translation, cell cycle, phosphorylation, signal transduction, immune response, RNA splicing/mRNA processing, and viral reproduction. The down-regulated genes were associated with xenobiotic/small molecule/lipid metabolic and oxidation–reduction processes. Hierarchical clustering of mRNAs and samples showed that samples from SVRs and relapsers clustered to form a group different from the null responders (Fig. S1). To validate the microarray results, qPCR was performed for all significant differentially expressed genes. The expression levels of MAP3K8 (mitogen-activated protein kinase kinase kinase 8, $p=5.24\times10^{-7}$), TMEM178 (transmembrane protein 178, $p=7.31\times10^{-6}$), PSME4 (proteasome activator subunit 4, also known as *PA200*, $p=2.43\times10^{-4}$), and EIF3B (eukaryotic translation initiation factor-3B, $p=3.16\times10^{-6}$; Fig. 1) were significantly increased in null/partial responders compared with those in SVRs/relapsers. TMEM178 is a multi-pass membrane protein and PSME4 is a nuclear protein that activates the proteasome and is important for oxidative-stress adaptation. EIF3B is involved in protein translation/synthesis and interacts with the HCV IRES and the 40S ribosomal subunit.

miRNAs associated with treatment response

miRNA microarray data were deposited into the NCBI GEO, accession number GSE45179. The cut-off criteria for fold change >1.2 and $p<0.005$ identified 111 down-regulated and 76 up-regulated miRNAs in null responders (Data S2). Hierarchical two-dimensional clustering showed that distinct patient groups clustered into two distinct groups (Fig. S2). Bioinformatic analysis predicted target genes of the differentially expressed miRNAs. The hypothetical target genes should be MAP3K8, TMEM178, PSME4, and EIF3B. Furthermore, these miRNAs and mRNAs must have an inverse correlation between mRNA and miRNA microarray data. The microRNAs that satisfied the requirements were as follows: hsa-let-7g* and hsa-miR-17-5p, -20b, -297, -374b, -494, -602, -668, and -1297 for MAP3K8; hsa-miR-106b* and -122-5p for TMEM178; and hsa-miR-492 and -675-5p for PSME4. No corresponding miRNA was identified for EIF3B.

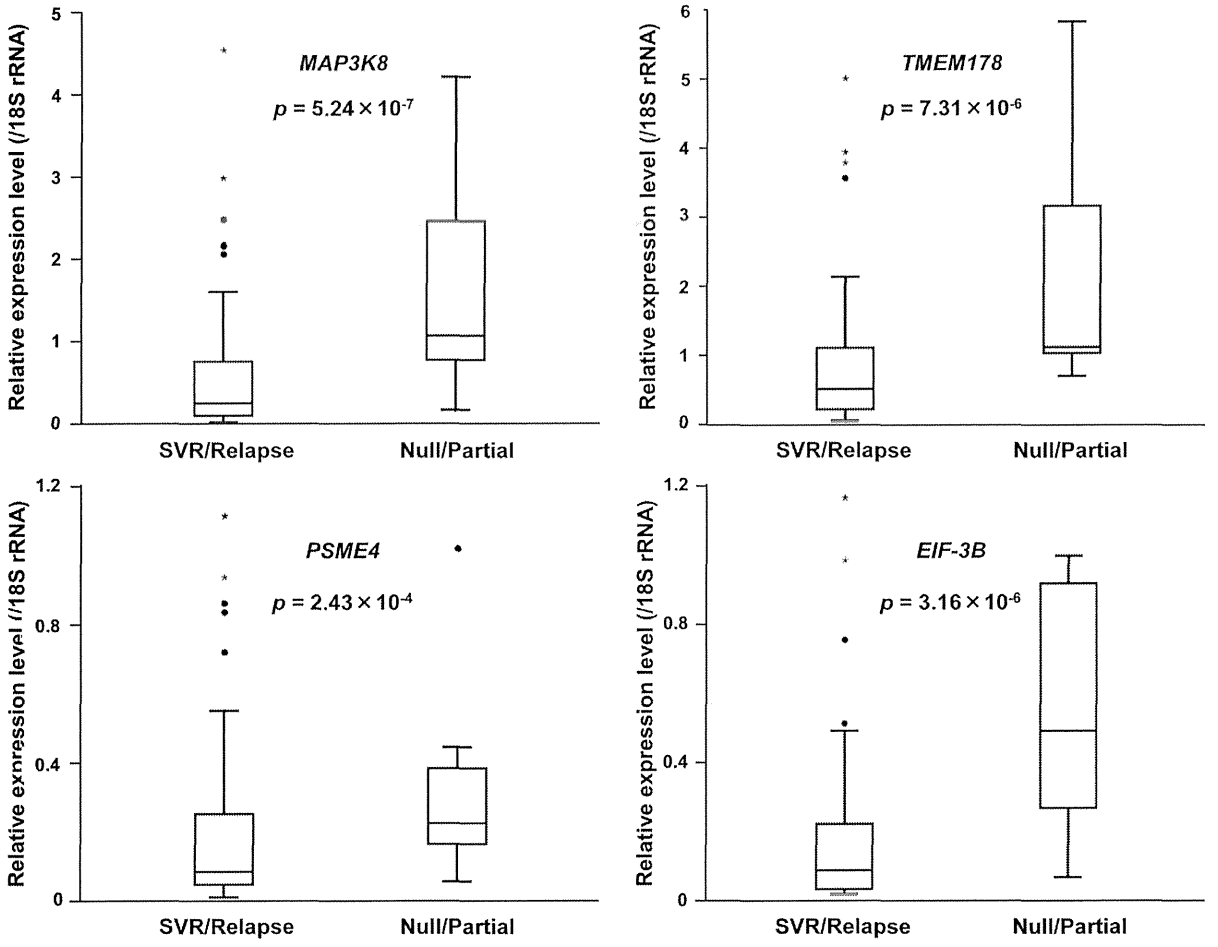

Figure 1. Validation of differentially expressed mRNAs by qPCR analysis. The expression levels of four mRNAs were significantly higher in null/partial responders than in SVRs/relapsers. Assays for each sample were performed in triplicate. All *p*-values were calculated using the Mann–Whitney test.
doi:10.1371/journal.pone.0097078.g001

Stem-loop-based qPCR was performed to confirm the reliability of the miRNA microarray results and the inverse correlation between miRNA and mRNA. The expression levels of hsa-miR-122-5p ($p = 2.75 \times 10^{-8}$), hsa-miR-675-5p ($p = 1.00 \times 10^{-5}$), and hsa-miR-17-5p ($p = 1.73 \times 10^{-8}$) were significantly lower in null/partial responders than in SVRs/relapsers (Fig. 2).

Independent variables associated with treatment response

Multiple logistic regression analysis of variables that were significant in univariate analysis identified that rs8099917 [$p = 3.67 \times 10^{-3}$, odds ratio (OR) = 7.51, 95% confidence interval (CI) = 2.14–29.27], hsa-miR-122-5p ($p = 5.60 \times 10^{-4}$, OR = 0.11, 95% CI = 0.03–0.38), hsa-miR-17-5p ($p = 2.02 \times 10^{-4}$, OR = 0.56, 95% CI = 0.41–0.76), and MAP3K8 ($p = 8.58 \times 10^{-3}$, OR = 2.86, 95% CI = 1.31–6.25) were significantly associated with null/partial response. Importantly, *in silico* analysis and microarray data suggested that increased miR-17-5p could cause MAP3K8 reduction. In fact, an inverse correlation was observed between MAP3K8 mRNA and miR-17-5p ($r = -0.592$, $p = 4.31 \times 10^{-3}$). MAP3K8 is closely linked to genes associated with cell proliferation, inflammation, and apoptosis (Fig. S3) and is associated with the miR-17 cluster family (Fig. S4).

MAP3K8 contributes to HCV production

siRNA transfection in HCVcc-infected cells was performed to assess the influence of MAP3K8 mRNA and protein on HCV production (Fig. 3A). miR-17-5p levels were significantly increased (Fig. 3B) while supernatant HCV core antigen levels were significantly decreased following transfection of the siRNAs (Fig. 3C). However, the HCV core antigen levels in cell lysates were not changed (Fig. 3C). Taken together, these findings suggested that MAP3K8 repressed miR-17-5p and contributed to the production (e.g. release and assembly) of HCV. *In vivo*, MAP3K8 protein expression levels were significantly increased in null/partial responders compared with those in SVRs/relapsers ($p = 2.43 \times 10^{-5}$).

Hsa-miR-17-5p regulates HCV production by targeting MAP3K8

Changes in MAP3K8 and HCV core antigen levels were evaluated by hsa-miR-17-5p inhibition and overexpression in HCVcc-infected cells. miR-17-5p inhibition increased MAP3K8 mRNA and protein levels (Fig. 4A and 4B, left). In contrast, miR-17-5p overexpression decreased MAP3K8 mRNA and protein levels (Fig. 4A and 4B, right). Interestingly, miR-17-5p inhibition increased, whereas miR-17-5p overexpression decreased HCV core antigen levels in both supernatants and cell lysates (Fig. 4C).

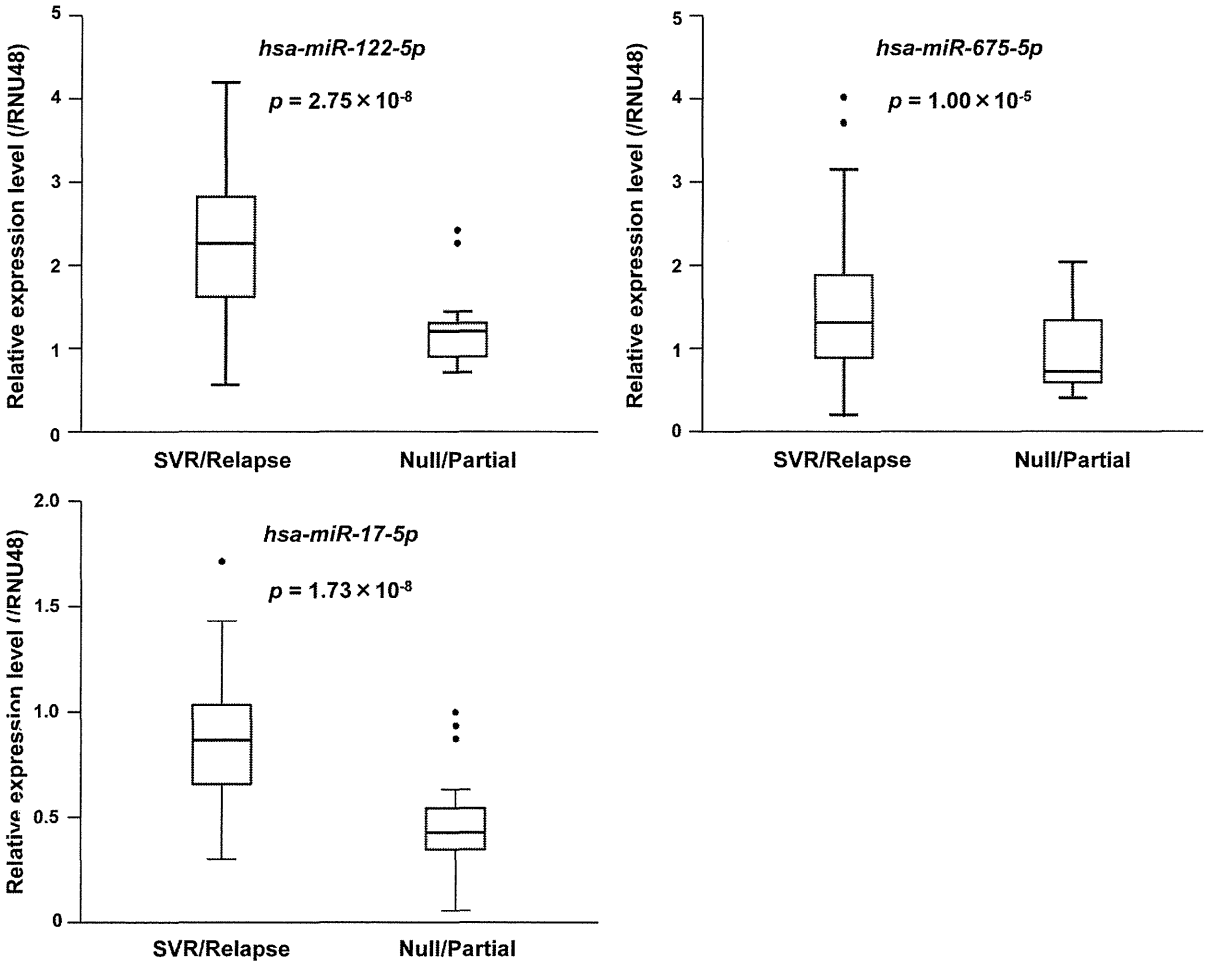

Figure 2. Validation of differentially expressed miRNAs by qPCR analysis. The expression levels of three miRNAs were significantly higher in null/partial responders than in SVRs/relapsers. Assays for each sample were performed in triplicate. All *p*-values were calculated using the Mann–Whitney test.
doi:10.1371/journal.pone.0097078.g002

Taken together, these results suggested that miR-17-5p regulated the production of HCV by targeting MAP3K8 mRNA. Luciferase reporter assays showed that miR-17-5p overexpression decreased the luciferase activity of the wild-type MAP3K8 3′UTR reporter construct, whereas co-transfection with the mutant MAP3K8 3′UTR construct or mock had no effect (Fig. 5), suggesting that miR-17-5p targeted the MAP3K8 3′UTR and antagonized MAP3K8 protein expression.

Discussion

This study showed close linkage between mRNA and miRNA signatures in CH-C treatment outcomes using global expression profiling analyses. To confirm the findings, this cohort was randomly divided into derivation and confirmatory groups. The derivation group results were similar to those described above and reproducible in the confirmatory group (data not shown). Subsequently, we attempted to compare our findings with registered patient data obtained from independent cohorts comprising either Asian or non-Asian subjects. However, comparisons were not possible because most mRNA or miRNA microarray studies had a small sample size, limited information, unregistered data, and/or findings that were not validated in an independent cohort [4–7,11,19–21]. To our knowledge, our study was the first to investigate the correlation between mRNA and miRNA in treatment response using global gene expression analysis and *in vitro* experiments. Such gene signature identification can improve the accuracy of treatment outcome predictions, independent of known strong predictors.

Pretreatment hepatic ISG levels are higher in non-SVRs/non-relapsers than in SVRs/relapsers [4–7]. The poor ISG response of non-SVRs with further exogenous IFN may contribute to treatment failure [5,6]. Because patient groups with different response categories differ in their innate IFN response to HCV infection; poor responders may have adopted a different equilibrium in their innate immune response to HCV [4,6]. As per multivariate regression analysis, however, IL28B SNPs may diminish the significance of hepatic ISGs as treatment predictors because hepatic ISG expression is associated with IL28B SNPs [7,19]. Conversely, hepatic ISGs were reported to be stronger predictors compared with IL28B SNPs [20]. Although our gene set enrichment analysis (data not shown) also showed that hepatic ISG expression levels were generally higher in null/partial responders than in SVRs/relapsers, the differences were not large enough to be ranked in a higher order and/or to reach statistical significance in expression profiling and validation analyses (Data S3). These variations among studies may be caused by different and heterogeneous patient characteristics, including HCV geno-

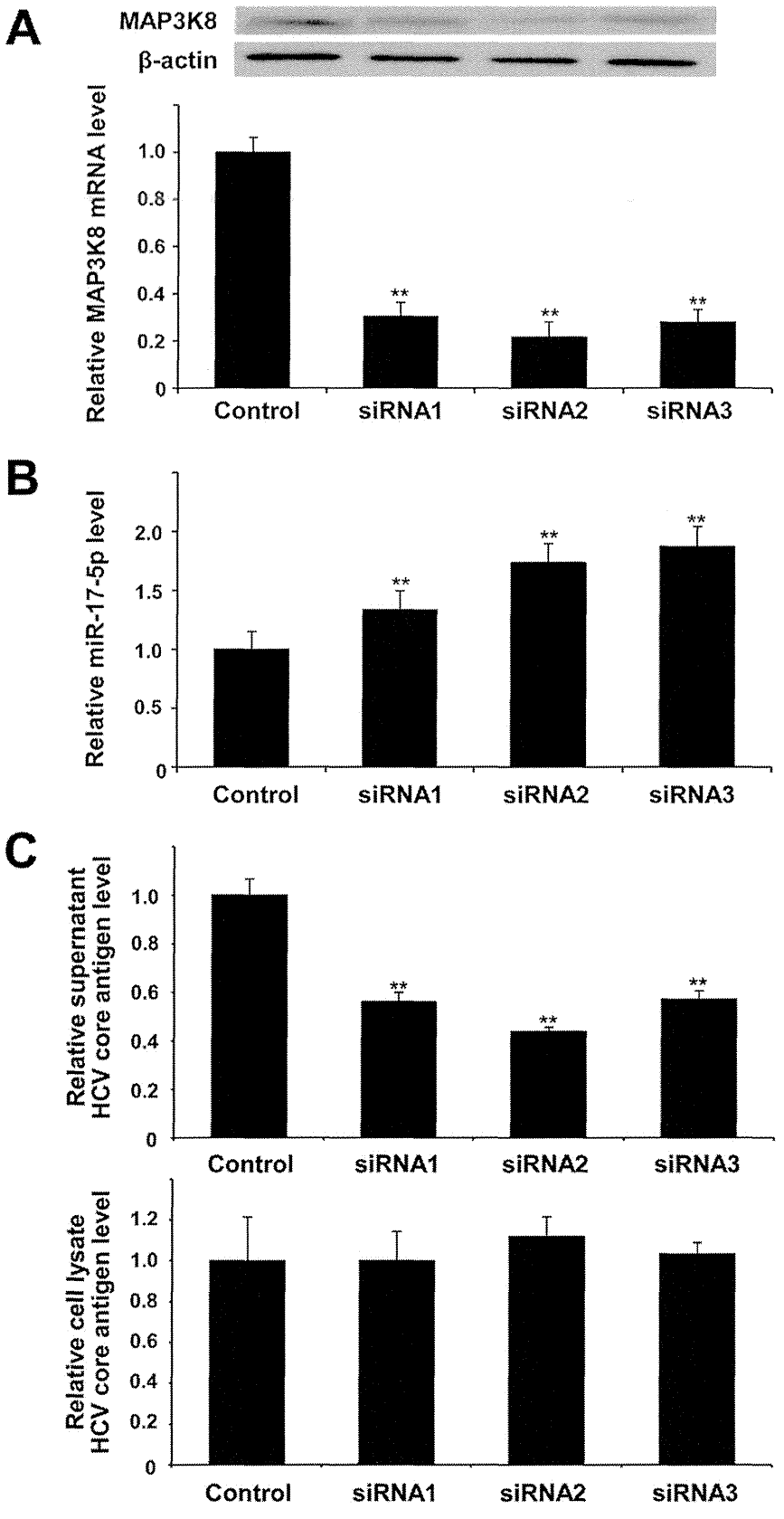

Figure 3. Transfection of Huh7.5.1 cells with siRNAs against MAP3K8. (**A**) Transfection of Huh7.5.1 cells with siRNAs against MAP3K8 significantly decreased intracellular MAP3K8 mRNA levels, (**B**) increased intracellular hsa-miR-17-5p levels, and (**C**) decreased HCV core antigen levels in the supernatant, and had no effect on those in cell lysate. Bars indicate the means of three independent experiments and the error bars indicate standard deviations. All *p*-values were calculated using two-tailed Student's *t*-test. $^{**}p<0.001$ compared with controls.
doi:10.1371/journal.pone.0097078.g003

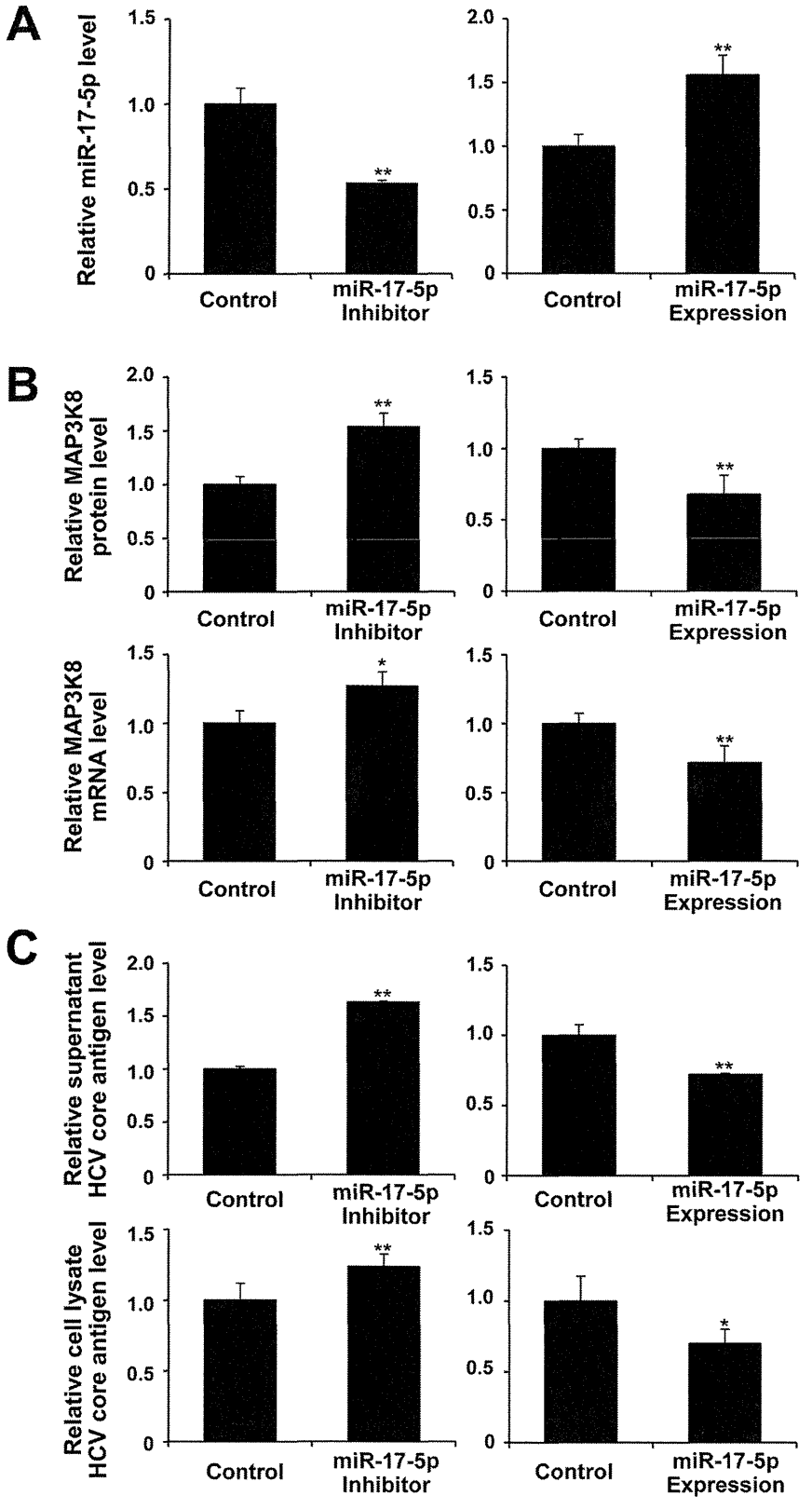

Figure 4. Expression and inhibition of hsa-miR-17-5p in Huh7.5.1 cells. (**A**) Functional suppression (left) and overexpression (right) plasmids of miR-17-5p. (**B**) Inhibition of miR-17-5p increased (left), whereas overexpression of miR-17-5p decreased MAP3K8 mRNA and protein expression levels (right). (**C**) HCV core antigen levels increased following miR-17-5p inhibition (left) and decreased by miR-17-5p overexpression (right) in both supernatant and cell lysate. Bars indicate the means of three independent experiments and the error bars indicate standard deviations. *$p<0.01$ and **$p<0.001$ compared with controls.
doi:10.1371/journal.pone.0097078.g004

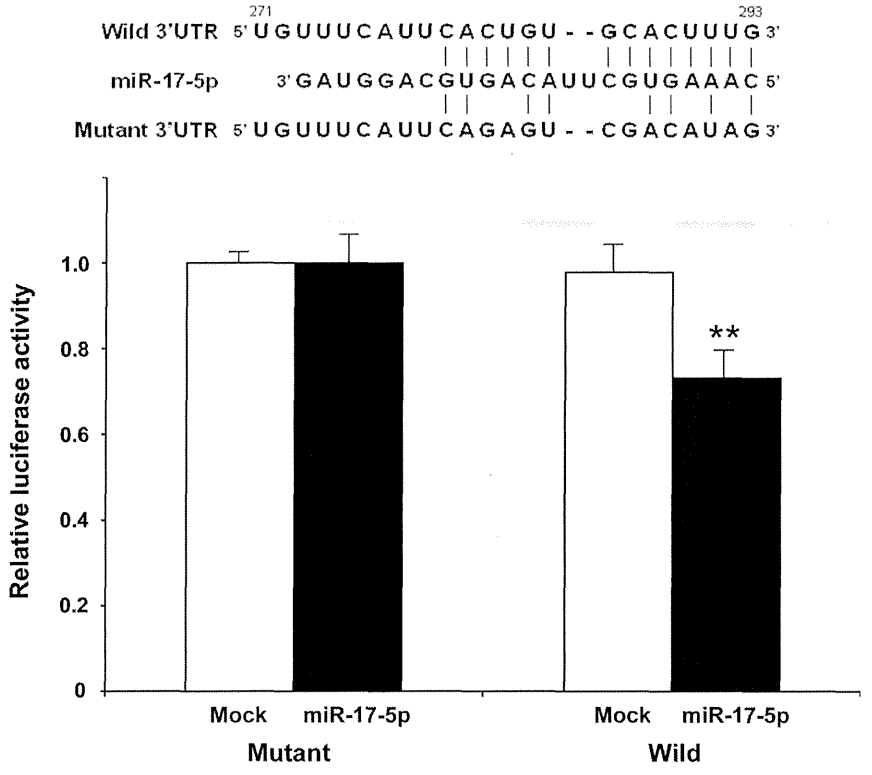

Figure 5. Luciferase reporter assay. miR-17-5p inhibited the luciferase activity of the wild-type MAP3K8 3'UTR construct (right), whereas no decrease in activity was observed in cells co-transfected with the mutant MAP3K8 3'UTR construct (left) or mock plus wild-type or mutant construct (right and left, respectively). Bars indicate the means of three independent experiments, and the error bars indicate standard deviations. $^{**}p<0.001$ compared with controls.
doi:10.1371/journal.pone.0097078.g005

type, patient race, treatment response definitions, study endpoints, and treatment regimens. This study analyzed patients with a homogeneous race and genotype (1b) who adhered to combination therapy and treatment for a specified duration.

MAP3K8, also known as cancer Osaka thyroid (cot) [22] or tumor progression locus 2 (tpl2) [23], was originally recognized as a proto-oncogenic protein. Toll-like receptors (TLRs) are innate immune sensors stimulated by specific microbial and viral components, including HCV. *In vitro* HCV infection directly induces TLR4 expression and activates human B cells to increase the production of IFN-β and IL-6 [24]. Peripheral blood mononuclear cells from HCV-infected individuals express higher TLR4 levels compared with uninfected controls [24]. In the IKK-NF-κB pathway, certain activated TLRs, including TLR4, induce inhibition of kappa B kinase (IKK)- catalyzed phosphorylation of nuclear factor kappa B (NF-κB) p105. Nonphosphorylated NF-κB p105 forms a stable, inactive complex with MAP3K8. Subsequent ubiquitination and proteasome-mediated processing of NF-κB-p105 to NF-κB-p50 releases MAP3K8, which activates the MAPK/ERK kinase (MEK)-extracellular signal-regulated kinase (ERK) pathway. MEK-ERK regulates the expression of pro- and anti-inflammatory mediators that lead to the production of various cytokines and chemokines in a stimulus- and cell/receptor type-specific manner (Fig. S3, Fig. S4) [25,26]. Indeed, MAP3K8 is an important and novel therapeutic target for inflammatory diseases [27]. MAP3K8 is involved in ERK signaling activation in hepatic Kupffer and stellate cells with being stimulated by TLR4 and TLR9, leading to ERK-dependent expression of the fibrogenic genes IL-1β and TIMP-1. Thus, MAP3K8 expression may contribute to liver fibrosis [28].

In addition, this study provided a novel insight into MAP3K8, which is involved in resistance to HCV treatment. The results of experiments in this study demonstrated the importance of MAP3K8 in HCV production. MAP3K8 knockdown by siRNA altered extracellular, but not intracellular, HCV core antigen levels. This result suggests that MAP3K8 might be involved in the release or assembly of HCV, does not exclude the possibility that MAP3K8 participates in intracellular HCV core production because miR-17-5p influenced both supernatant and cell-lysate HCV core antigen levels along with MAP3K8 mRNA and protein levels. If MAP3K8 limited viral release/assembly alone, intracellular HCV core antigen would accumulate following siRNA transfection. Conversely, MAP3K8 overexpression did not affect HCV production, probably because enough MAP3K8 may exist in the cells. This result is generally observed in other critical host factors (e.g. hVAP-33) involved in the HCV life cycle [29]. The above description [24–26] and *in silico* analyses (Fig. S3, Fig. S4) suggest that MAP3K8 might play a role in HCV production through a regulatory pathway and network (Fig. S5); however, the exact mechanism remains unknown and requires further investigation. It is important to note that there may be differences between the HCV genotype 1b- and 2a-derived strains/replicons. The 2a-derived JFH1 infection system is highly competent compared with other genotype-derived systems and allows steady inhibition and expression analyses [30]. Notably, this *in vitro* study focused on the correlation between MAP3K8 and miR-17-5p and their impact on HCV production; there may not be significant genotypic effect on MAP3K8 and miR-17-5p. Importantly, it is difficult to determine genotype-specific differences using different infection-competent systems.

The miR-17-92 polycistron, also known as the first oncomir, encodes six or seven miRNAs, including miR-17-5p [31,32], and is frequently overexpressed in several tumors [31,33]. In contrast, overexpression of miR-17-5p also leads to tumor suppression in breast cancer [34] and HeLa cells [32]. miR-17-5p may function as both a tumor suppressor and an oncogenic activator by targeting both pro- and anti-proliferative genes and by competing with each other in different cellular contexts, which are dependent on the expression of other transcriptional regulators [35]. Known targets of the miR-17-92 cluster primarily regulate cell cycle progression, apoptosis, and transcription factors [32,35]. Physiologically, this cluster is down-regulated during aging, and hematopoietic and lung differentiation. During HIV infection, suppression of this cluster by the virus is required for efficient viral replication [36]. Our results suggest that inhibition of miR-17-5p expression may be advantageous for HCV production. Interestingly, miR-17-5p overexpression in HeLa cells decreases the expression of the low-density lipoprotein (LDL) receptor (LDLR) and consequently induces reduced intracellular lipoprotein accumulation because of the impaired internalization [32]. LDLR is one of putative HCV receptors; however, its precise role remains controversial [37-40]. LDLR also aids the optimization of HCV replication, and the expression levels are stimulated by HCV infection. Decreased LDLR and lipoprotein uptake through LDLR may adversely affect the HCV life cycle because hepatocyte lipid metabolism pathways are required for HCV.

Bioinformatics and *in vitro* experiments showed that miR-17-5p expression levels were inversely correlated with MAP3K8 in response to anti-HCV treatment. miR-17-5p repressed HCV production by inhibiting MAP3K8 expression, whereas miR-17-5p expression was influenced by MAP3K8. The results also suggested a specific interaction between miR-17-5p and MAP3K8 3′UTR, which was previously validated by the luciferase reporter assay [35]. Taken together, MAP3K8 expression following HCV infection is negatively influenced by miR-17-5p at both the translational and transcriptional levels. This molecular interaction is a potential target for novel molecular therapeutics. However, a single miRNA can regulate the expression of multiple target mRNAs by imperfect base pairing [9,10]. Conversely, the expression of a single mRNA may be regulated by several miRNAs. Numerous mRNAs and miRNAs are key regulators in complicated pathophysiological networks (Fig. S3, Fig. S4). Therefore, it is important to note that the complex interaction between MAP3K8 and miR-17-5p may not be reflective of a correlation between their expression and viral load in our patient cohort.

Abundant hepatic miR-122 expression is essential for efficient HCV replication in cultured human hepatoma cells [11]. Suppression of miR-122 leads to a marked reduction and long-lasting suppression of HCV RNA in both sera and the livers of nonhuman primates with chronic HCV infection [41]. Paradoxically, this study showed significantly lower miRNA-122 (hsa-miR-122-5p) expression levels in null/partial responders than in SVRs/relapsers, independent of other factors. This finding is in agreement with the results of a previous study, which reported markedly low baseline miR-122 levels in poor responders [21]. Moreover, no positive correlation was observed between miR-122 expression and viral load. No convincing explanation exists for these paradoxical results. Re-analysis of registered miRNA microarray data [8] identified significantly low miR-122 levels, no change in miR-675-5p levels, and low (although not significant) miR-17-5p levels in null/partial responders. Most miR-122 target genes are involved in the lipid biogenesis pathway [42], and miR-122 antagonism induces a substantial decrease in plasma lipid levels. As described above, host lipid metabolism is vital to HCV [40], and may be related to the endogenous IFN response to HCV and IL28B SNPs [43]. However, we did not find a correlation between miR-122 expression and serum lipid levels nor identify miR-122 target genes, including lipid-related metabolic pathways, which could be considered key molecular signatures contributing to a null/partial response.

In conclusion, both global mRNA and miRNA expression profiling analyses increase our understanding of the molecular mechanisms that underlie refractory treatment responses and are even applicable to next-generation treatment. The results obtained in this study also aid the identification of novel features of known genes and target molecules for future therapeutic intervention.

Supporting Information

Figure S1 Hierarchical cluster analysis of mRNA expression using microarray analysis. Changes in mRNA expression levels are presented in graduated color patches from green (least expression) to red (most abundant expression).
(TIF)

Figure S2 Hierarchical cluster analysis of miRNA expression using microarray analysis. Changes in gene expression are presented in graduated color patches from blue (least expression) to red (most abundant expression).
(TIF)

Figure S3 Relationship between MAP3K8 (Tpl2/Cot) and related genes in underlying gene regulatory networks. MAP3K8 (Tpl2/Cot) was integrated by Kyoto Encyclopedia of Genes and Genomes (KEGG) Pathways. MAP3K8 (Tpl2/Cot) was identified as an important node and considered to be a key regulator.
(TIF)

Figure S4 Gene networks for MAP3K8 and hsa-miR-17. MAP3K8 and hsa-miR-17 and array-independent/literature-based text-mining were integrated into the gene regulatory network analysis (Agilent Literature Search). The interaction data were visualized and analyzed by Cytoscape. MAP3K8 and its related mRNAs were associated with the miR-17 cluster family and its related miRNAs via IRF6, STAT3, AKT1, EPHB2, TIMP1, and VEGFA.
(TIF)

Figure S5 Postulated scheme for HCV replication regulated by MAP3K8 and hsa-miR-17-5p. IKK, inhibition of kappa B kinase; NF-κB, nuclear factor kappa B; MAP3K8, mitogen-activated protein kinase kinase kinase 8; MEK, MAPK/extracellular signal-regulated kinase.
(TIF)

Table S1 Comparison of baseline profiles between SVRs/relapsers and null/partial responders.
(DOC)

Data S1 List of gene probe sets up- and down-regulated in sustained virological responders (SVR) and relapsers compared with those in null responders.
(XLS)

Data S2 List of microRNA probe sets up- and down-regulated in sustained virological responders (SVR) and relapsers compared with those in null responders.
(XLS)

Data S3 List of all gene probe sets up- and down-regulated in sustained virological responders (SVR) and

relapsers compared with those in null responders, and gene signatures in previously reported references.
(XLS)

Acknowledgments

We thank Dr. Takaji Wakita (National Institute of Infectious Diseases) for providing the JFH1-transfected cells and Haruyo Aoyagi (National Institute of Infectious Diseases), Ric Agata, and Yoko Yumoto (Jikei University School of Medicine) for their excellent technical support.

Author Contributions

Conceived and designed the experiments: AT HA. Performed the experiments: AT HA K. Miyaguchi. Analyzed the data: AT K. Mogushi HA K. Miyaguchi TK TF HT. Contributed reagents/materials/analysis tools: AT KN HM TM TF. Wrote the paper: AT.

References

1. Ghany MG, Nelson DR, Strader DB, Thomas DL, Seeff LB (2011) An update on treatment of genotype 1 chronic hepatitis C virus infection: 2011 practice guideline by the American Association for the Study of Liver Diseases. Hepatology 54: 1433–1444.
2. Kumada H, Toyota J, Okanoue T, Chayama K, Tsubouchi H, et al. (2012) Telaprevir with peginterferon and ribavirin for treatment-naive patients chronically infected with HCV of genotype 1 in Japan. J Hepatol 56: 78–84.
3. Hayashi N, Okanoue T, Tsubouchi H, Toyota J, Chayama K, et al. (2012) Efficacy and safety of telaprevir, a new protease inhibitor, for difficult-to-treat patients with genotype 1 chronic hepatitis C. J Viral Hepat 19: e134–142.
4. Chen L, Borozan I, Feld J, Sun J, Tannis LL, et al. (2005) Hepatic gene expression discriminates responders and nonresponders in treatment of chronic hepatitis C viral infection. Gastroenterology 128: 1437–1444.
5. Feld JJ, Nanda S, Huang Y, Chen W, Cam M, et al. (2007) Hepatic gene expression during treatment with peginterferon and ribavirin: Identifying molecular pathways for treatment response. Hepatology 46: 1548–1563.
6. Sarasin-Filipowicz M, Oakeley EJ, Duong FH, Christen V, Terracciano L, et al. (2008) Interferon signaling and treatment outcome in chronic hepatitis C. Proc Natl Acad Sci USA 105: 7034–7039.
7. Honda M, Sakai A, Yamashita T, Nakamoto Y, Mizukoshi E, et al. (2010) Hepatic ISG expression is associated with genetic variation in interleukin 28B and the outcome of IFN therapy for chronic hepatitis C. Gastroenterology 139: 499–509.
8. Murakami Y, Tanaka M, Toyoda H, Hayashi K, Kuroda M, et al. (2010) Hepatic microRNA expression is associated with the response to interferon treatment of chronic hepatitis C. BMC Med Genomics 3: 48.
9. Lim LP, Lau NC, Garrett-Engele P, Grimson A, Schelter JM, et al. (2005) Microarray analysis shows that some microRNAs downregulate large numbers of target mRNAs. Nature 433: 769–773.
10. Selbach M, Schwänhausser B, Thierfelder N, Fang Z, Khanin R, et al. (2008) Widespread changes in protein synthesis induced by microRNAs. Nature 455: 58–63.
11. Jopling CL, Yi M, Lancaster AM, Lemon SM, Sarnow P (2005) Modulation of hepatitis C virus RNA abundance by a liver-specific MicroRNA. Science 309: 1577–1581.
12. Gottwein E, Cullen BR (2008) Viral and cellular microRNAs as determinants of viral pathogenesis and immunity. Cell Host Microbe 3: 375–387.
13. Desmet VJ, Gerber M, Hoofnagle JH, Manns M, Scheuer PJ (1994) Classification of chronic hepatitis: diagnosis, grading and staging. Hepatology 19: 1513–1520.
14. Zhong J, Gastaminza P, Cheng G, Kapadia S, Kato T, et al. (2005) Robust hepatitis C virus infection in vitro. Proc Natl Acad Sci USA 102: 9294–9299.
15. Wakita T, Pietschmann T, Kato T, Date T, Miyamoto M, et al. (2005) Production of infectious hepatitis C virus in tissue culture from a cloned viral genome. Nat Med 11: 791–796.
16. Ge D, Fellay J, Thompson AJ, Simon JS, Shianna KV, et al. (2009) Genetic variation in IL28B predicts hepatitis C treatment-induced viral clearance. Nature 461: 399–401.
17. Tanaka Y, Nishida N, Sugiyama M, Kurosaki M, Matsuura K, et al. (2009) Genome-wide association of IL28B with response to pegylated interferon-alpha and ribavirin therapy for chronic hepatitis C. Nat Genet 41: 1105–1109.
18. Fellay J, Thompson AJ, Ge D, Gumbs CE, Urban TJ, et al. (2010) ITPA gene variants protect against anaemia in patients treated for chronic hepatitis C. Nature 464: 405–408.
19. Urban TJ, Thompson AJ, Bradric SS, Fellay J, Schuppan D, et al. (2010) IL28B genotype is associated with differential expression of intrahepatic interferon-stimulated genes in patients with chronic hepatitis C. Hepatology 52: 1888–1896.
20. Dill MT, Duong FHT, Vogt JE, Bibert S, Bochud PY, et al. (2011) Interferon-induced gene expression is a stronger predictor of treatment response than IL28B genotype in patients with hepatitis C. Gastroenterology 140: 1021–1031.
21. Sarasin-Filipowicz M, Krol J, Markiewicz I, Heim MH, Filipowicz W (2009) Decreased levels of microRNA miR-122 in individuals with hepatitis C responding poorly to interferon therapy. Nat Med 15: 31–33.
22. Miyoshi J, Higashi T, Mukai H, Ohuchi T, Kakunaga T (1991) Structure and transforming potential of the human cot oncogene encoding a putative protein kinase. Mol Cell Biol 11: 4088–4096.
23. Patriotis C, Makris A, Bear SE, Tsichlis PN (1993) Tumor progression locus 2 (Tpl-2) encodes a protein kinase involved in the progression of rodent T-cell lymphomas and in T-cell activation. Proc Natl Acad Sci USA 90: 2251–2255.
24. Machida K, Cheng KT, Sung VM, Levine AM, Foung S, et al. (2006) Hepatitis C virus induces toll-like receptor 4 expression, leading to enhanced production of beta interferon and interleukin-6. J Virol 80: 866–874.
25. Banerjee A, Gerondakis S (2007) Coordinating TLR-activated signaling pathways in cells of the immune system. Immunol Cell Biol 85: 420–424.
26. Gantke T, Sriskantharajah S, Sadowski M, Ley SC (2012) IκB kinase regulation of the TPL-2/ERK MAPK pathway. Immunol Rev 246: 168–182.
27. George D, Salmeron A (2009) Cot/Tpl-2 protein kinase as a target for the treatment of inflammatory disease. Curr Top Med Chem 9: 611–622.
28. Perugorria MJ, Murphy LB, Fullard N, Chakraborty JB, Vyrla D, et al. (2013) Tpl2/Cot is required for activation of ERK in liver injury and TLR induced TIMP-1 gene transcription in hepatic stellate cells. Hepatology 57: 1238–1249.
29. Gao L, Aizaki H, He JW, Lai MM (2004) Interactions between viral nonstructural proteins and host protein hVAP-33 mediate the formation of hepatitis C virus RNA replication complex on lipid raft. J Virol 78: 3480–3488.
30. Kato T, Matsumura T, Heller T, Saito S, Sapp RK, et al. (2007) Production of infectious hepatitis C virus of various genotypes in cell cultures. J Virol 81: 4405–4411.
31. He L, Thomson JM, Hemann MT, Hernando-Monge E, Mu D, et al. (2005) A microRNA polycistron as a potential human oncogene. Nature 435: 828–833.
32. Serva A, Knapp B, Tsai YT, Claas C, Lisauskas T, et al. (2012) miR-17-5p regulates endocytic trafficking through targeting TBC1D2/Armus. PLoS One 7: e52555.
33. Volinia S, Calin GA, Liu CG, Ambs S, Cimmino A, et al. (2006) A microRNA expression signature of human solid tumors defines cancer gene targets. Proc Natl Acad Sci USA 103: 2257–2261.
34. Hossain A, Kuo MT, Saunders GF (2006) Mir-17-5p regulates breast cancer cell proliferation by inhibiting translation of AIB1 mRNA. Mol Cell Biol 26: 8191–8201.
35. Cloonan N, Brown MK, Steptoe AL, Wani S, Chan WL, et al. (2008) The miR-17-5p microRNA is a key regulator of the G1/S phase cell cycle transition. Genome Biol 9: R127.
36. Triboulet R, Mari B, Lin YL, Chable-Bessia C, Bennasser Y, et al. (2007) Suppression of microRNA-silencing pathway by HIV-1 during virus replication. Science 315: 1579–1582.
37. Albecka A, Belouzard S, Op de Beeck A, Descamps V, Goueslain L, et al. (2012) Role of low-density lipoprotein receptor in the hepatitis C virus life cycle. Hepatology 55: 998–1007.
38. Bassendine MF, Sheridan DA, Bridge SH, Felmlee DJ, Neely RD (2013) Lipids and HCV. Semin Immunopathol 35: 87–100.
39. Schaefer EA, Chung RT (2013) HCV and host lipids: an intimate connection. Semin Liver Dis 33: 358–368.
40. Syed GH, Tang H, Khan M, Hassanein T, Liu J, et al. (2014) Hepatitis C virus stimulates low-density lipoprotein receptor expression to facilitate viral propagation. J Virol 88: 2519–2529.
41. Lanford RE, Hildebrandt-Eriksen ES, Petri A, Persson R, Lindow M, et al. (2010) Therapeutic silencing of microRNA-122 in primates with chronic hepatitis C virus infection. Science 327: 198–201.
42. Krützfeldt J, Rajewsky N, Braich R, Rajeev KG, Tuschl T, et al. (2005) Silencing of microRNAs in vivo with 'antagomirs'. Nature 438: 685–689.
43. Li JH, Lao XQ, Tillmann HL, Rowell J, Patel K, et al. (2010) Interferon-lambda genotype and low serum low-density lipoprotein cholesterol levels in patients with chronic hepatitis C infection. Hepatology 51: 1904–1911.